The Mechanism of Spectral Shift and Inhomogeneous Broadening of an Aromatic Chromophore in a Polymer Glass

Epameinondas Leontidis,[†] Ulrich W. Suter,*[,†] Martin Schütz,[‡] Hans-Peter Lüthi,[‡] Alois Renn,[§] and Urs P. Wild[§]

Contribution from the Institute of Polymers, Interdisciplinary Project-Center for Supercomputing, and Physical Chemistry Laboratory, ETH Zentrum, CH-8092 Zürich, Switzerland

Received December 19, 1994[⊗]

Abstract: We have attempted to obtain microscopic-level understanding of the absorption band of the chromophore *s*-tetrazine in a glassy polymer matrix (atactic polypropylene) at low temperatures. Our investigation has focused on the bathochromic shift of the lowest-energy $\pi^* \leftarrow n$ ($^1B_{3u} \leftarrow {}^1A_g$) electronic transition of the chromophore in the polymer matrix as well as on the width of the inhomogeneously broadened absorption band. The absorption spectrum of *s*-tetrazine in atactic polypropylene was measured over a range of temperatures for comparison with modeling results. Information on the geometry and the electronic structure of *s*-tetrazine in the ground and excited states was obtained from ab initio calculations. We have generated several polymer microstructures with imbedded chromophore molecules and used classical *NpT* molecular dynamics simulations to obtain ground-state trajectories of the chromophore. The classical Franck−Condon principle was invoked to calculate the average solvent shift. The dominant dispersion contribution to the solvent shift was calculated both, using an empirical parametrization of pair-potentials for the excited state (Kettley et al. *Chem. Phys. Lett.* **1986**, *126*, 107−12) and using the semiempirical theory of Shalev et al. (*J. Chem. Phys.* **1991**, *95*, 3147−66). The very encouraging results obtained indicate that the concurrent use of ab initio calculations, semiempirical methods, and classical simulation techniques can provide valuable insights into the complex microscopic interactions in low-temperature amorphous materials. It is also anticipated that such computational investigations may become valuable supplements to line-narrowing and single-molecule spectroscopic investigations of amorphous polymers at low temperatures.

I. Introduction and Goals

Polymeric host-matrices have often been used in the past to study spectroscopic properties of small molecules and to investigate solvatochromic effects and local interactions in solid amorphous hosts.[1−15] The spectroscopy of organic chromophores in polymer matrices is increasingly attracting attention: Glassy polymer matrices are now regularly used in line-narrowing spectroscopy[3−12] and single-molecule spectroscopy.[13] The potential of persistent hole-burning spectroscopy for optical data storage,[8,14] and the detailed information on molecular interactions, offered by line-narrowing and single-molecule spectroscopy, render necessary the examination of polymer-chromophore systems at the microscopic level. To date, low-temperature spectroscopic investigations have involved a large variety of polymeric hosts and chromophores,[1−15] and a large body of experimental data has been collected. However, there has been no detailed theoretical or computational study of polymer-chromophore interactions.

The resolution of low-temperature spectroscopic techniques is currently limited by the homogeneous line width.[8,14c] From the point of view of applying hole-burning spectroscopy for optical data-storage (leaving aside a number of technical

[†] Institute of Polymers.

[‡] Interdisciplinary Project-Center for Supercomputing.

[§] Physical Chemistry Laboratory.

[⊗] Abstract published in *Advance ACS Abstracts,* June 15, 1995.

(1) Guillet, J. *Polymer Photophysics and Photochemistry*; Cambridge University Press: Cambridge, 1985.

(2) (a) Suppan, P. *J. Photochem. Photobiol., A: Chem.* **1990**, *50*, 293−330. (b) Cazeau-Dubroca, C.; Peirigua, A.; Ait Lyazidi, S.; Nouchi, G. *Chem. Phys. Lett.* **1983**, *98*, 511−514.

(3) (a) Bogner, U.; Beck, K.; Maier, M. *Appl. Phys. Lett.* **1985**, *46*, 534−536. (b) Maier, M. *Appl. Phys. B* **1986**, *41*, 73−90. (c) Gerblinger, J.; Bogner, U.; Maier, M. *Chem. Phys. Lett.* **1987**, *141*, 31−35. (d) Kanaan, Y.; Attenberger, T.; Bogner, U.; Maier, M. *Appl. Phys. B* **1990**, *51*, 336−341. (e) Hartmannsgruber, N.; Maier, M. *J. Chem. Phys.* **1992**, *96*, 7279−7286.

(4) (a) Meixner, A. J.; Renn, A.; Bucher, S. E.; Wild, U. P. *J. Phys. Chem.* **1986**, *90*, 6777−6785. (b) Meixner, A. J.; Renn, A.; Wild, U. P. *Chem. Phys. Lett.* **1992**, *190*, 75−82. (c) Vauthey, E.; Holliday, K.; Wei, C.; Renn, A.; Wild, U. P. *Chem. Phys.* **1993**, *171*, 253−263. (d) Vauthey, E.; Voss, J.; de Caro, C.; Renn, A.; Wild, U. P. *Chem. Phys.* **1994**, *184*, 347−56.

(5) (a) Kador, L.; Schulte, G.; Haarer, D. *J. Phys. Chem.* **1986**, *90*, 1264−1270. (b) Kador, L.; Haarer, D.; Personov, R. *J. Chem. Phys.* **1987**, *86*, 5300−5307. (c) Kador, L.; Jahn, S.; Haarer, D.; Silbey, R. *Phys. Rev. B* **1990**, *41*, 12215−12226. (d) Altmann, R. B.; Renge, I.; Kador, L.; Haarer, D. *J. Chem. Phys.* **1992**, *97*, 5316−5322.

(6) (a) Friedrich, J.; Haarer, D. *Angew. Chem., Int. Ed. Engl.* **1984**, *23*, 113−140. (b) Haarer, D.; Silbey, R. *Physics Today* **1990**, May issue, 58−65.

(7) (a) Jankowiak, R.; Small, G. J. *Science* **1987**, *237*, 618−625. (b) Jankowiak, R.; Hayes, J. M.; Small, G. J. *Chem. Rev.* **1993**, *93*, 1471−1502.

(8) Moerner, W. E., Ed.; *Topics in Current Physics, Persistent Spectral Hole Burning: Science and Applications*; Springer-Verlag: New York, 1987; Vol. 44.

(9) (a) Völker, S. *Ann. Rev. Phys. Chem.* **1989**, *40*, 499−530. (b) Thijssen, H. P. H.; Van den Berg, R.; Völker, S. *Chem. Phys. Lett.* **1983**, *97*, 295−302. (c) Thijssen, H. P. H.; Völker, S. *Chem. Phys. Lett.* **1985**, *120*, 496−502.

(10) Thijssen, H. P. H.; Völker, S. *J. Chem. Phys.* **1986**, *85*, 785.

(11) (a) Narasimhan, L. R.; Littau, K. A.; Pack, D. W.; Bai, Y. S.; Elschner, A.; Fayer, M. D. *Chem. Rev.* **1990**, *90*, 439−457. (b) Berg, M.; Walsh, C. A.; Narasimhan, L. R.; Littau, K. A.; Fayer, M. D. *J. Chem. Phys.* **1988**, *88*, 1564−1587.

(12) Molenkamp, L. W.; Wiersma, D. A. *J. Chem. Phys.* **1985**, *83*, 1−9.

(13) (a) Moerner, W. E.; Basché, T. *Angew. Chem., Int. Ed. Engl.* **1993**, *32*, 457−476. (b) Orrit, M.; Bernard, J.; Personov, R. I. *J. Phys. Chem.* **1993**, *97*, 10256−10268. (c) Myers, A. B.; Tchénio, P.; Zgierski, M. Z.; Moerner, W. E. *J. Phys. Chem.* **1994**, *94*, 10377−10390.

(14) (a) Renn, A.; Wild, U. P. *Appl. Opt.* **1987**, *26*, 4040−4042. (b) Wild, U. P.; De Caro, C.; Bernet, S.; Traber, M.; Renn, A. *J. Lumin.* **1991**, 335−339. (c) Wild, U. P.; Rebane, A.; Renn, A. *Adv. Mater.* **1991**, *3*, 453−456.

(15) Kettner, R.; Tittel, J.; Basché, Th.; Bräuchle, C. *J. Phys. Chem.* **1994**, 6671−6674.

0002-7863/95/1517-7493$09.00/0

problems), it is important to understand and control precisely the factors that contribute to the homogeneous and inhomogeneous line widths of absorption bands of chromophores in glassy polymers. A variety of nonspecific (dispersion, induction, direct multipole) and specific (hydrogen-bonding) interactions are active in the polar polymeric matrices that are typically used [e.g., poly(vinyl butyral),[3-5] poly(methyl methacrylate)[4,9]], and their relative importance must be assessed. On the other hand, polyethylene has been used as the host in most of the pioneering work involving single-molecule spectroscopy in polymers,[13] a notable exception being the very recent investigation of Kettner et al.[15] who used polyisobutylene. To develop detailed understanding of molecular interactions and spectral diffusion phenomena, polyethylene is an inappropriate host-matrix because of its significant crystallinity.[16] In fact, a recent theoretical investigation of spectral diffusion phenomena in solids has suggested that domain boundaries inside the material may be connected to spectral "jumps" in crystalline and semicrystalline hosts,[17] while previous experimental work had demonstrated that the width of the homogeneous absorption line depends on the crystallinity of the polymer.[10] Thus, in order to avoid interpretation problems, it is highly desirable to study purely amorphous host-matrices.

Several questions of a theoretical nature have been raised by the results of spectroscopic studies in polymers:

(1) For a specific *amorphous* polymer host and a specific *nonpolar* chromophore: What are the reasons for the solvent shift and the inhomogeneous broadening? Is there a correspondence, in this respect, between glassy polymers and liquid solvents? Can we explain (or—even better—predict or obtain a measure of) the sign and the magnitude of the spectral shift and the width of the inhomogeneously broadened band? Is the environment of the molecules that absorb at the edges of the absorption band "special" in any way?

(2) How does the nature of the polymer (polarizability, presence of polar groups, density) affect the spectral properties of a particular chromophore?

(3) What is the role of the electron density on the chromophore? How does the situation change when chromophores with permanent dipole moments are considered?

(4) Can single-molecule (homogeneous) line shapes for these systems be calculated? What is the effect of the environment and of temperature on the line shape? Can we observe spectral diffusion by modeling realistic systems? Would such studies help to identify the nature of the elusive two-level systems (TLSs)[7,8,11-13,17] in polymer glasses?

Here, we are primarily interested in understanding the solvent shift and the width of the absorption band for a specific polymer-chromophore system. The strategy of this investigation is to examine the impact of each specific or nonspecific interaction individually. As a first step we have found it profitable to start with a nonpolar chromophore (*s*-tetrazine) that has been extensively studied and characterized in the past and a specific nonpolar, completely amorphous polymer host (atactic polypropylene). Depending on the results of this investigation, it may become attractive to examine more polar polymeric hosts and finally extend the computations to dipolar chromophores. In essence, this is a feasibility study, being the first of its kind for atomistically detailed polymer glasses. Our goal is to show that a combination of classical molecular dynamics and semiempirical calculations may provide satisfactory estimates of both the solvent shift and the inhomogeneous distribution of the absorption bands of chromophores in polymer glasses without *going to an ambiguous continuum representation for the glassy solvent*. In addition, by treating the problem at the atomistic scale, we hope to obtain significant insights respecting the microscopic mechanisms that determine the inhomogeneous line width in a glassy polymer.

At the outset, we limit ourselves to an examination of the static spectrum only, considering the causes for inhomogeneous broadening that originate in the structural heterogeneities of the glassy polymer-chromophore system. Insight into the nature of two-level systems cannot be gained in this way, however.

In section II we present a short review of the theoretical and computational methods for modeling the solvatochromic shift and the inhomogeneous broadening of electronic absorption bands in solids. In section III we discuss the particular system chosen for the present investigation, and describe the ab initio calculations of the ground and excited states of *s*-tetrazine and the classical modeling of *s*-tetrazine using interatomic pair potentials and an empirical force field. The classical force field for polypropylene is also described here. Section IV contains a description of our experimental investigation of the absorption spectroscopy of *s*-tetrazine in polypropylene. In section V we describe in detail the computational methods used in the present study, namely, how the polymer-chromophore structures are created and how the solvent shift is obtained from these structures using classical molecular dynamics, the classical Franck–Condon principle, and the semiempirical theory of Shalev et al.,[18] respectively. Section VI contains the results we obtained by considering all possible mechanisms for the solvent shift. We first examine molecular distortion due to packing in the solid state and then consider the contribution of electrostatic interactions to the solvent shift. Finally, we discuss the dominant dispersion contribution to the solvent shift and take a closer look at the immediate solvating environment of a chromophore and the actual range of the interactions that determine the spectral shift. The last section contains a critical analysis and discussion of the results of section VI, our conclusions from the present investigation and directions for future work in this area.

II. Solvent Effects on Absorption Spectra: The State of the Art

II.1. Modeling of Solvatochromic Shifts. A vast amount of literature exists today on the effect of solvents on electronic (absorption and emission) spectra of chromophores.[19-23] It is generally observed that the absorption band of any electronic transition of any chromophore is shifted in a solvent with respect to its position in vacuum. The reason, recognized already in the early years of spectral-shift investigations,[24] is the different degree of stabilization (or destabilization) of the ground and excited states in the solvent, compared to their state in vacuo. The large body of available experimental results is supplemented by a variety of theoretical methods that have been used to correlate and explain the experimental data on solvatochromic shifts.[19-36] The initial attempts in this area were based on second-order perturbation theory[19,21,25,26,28] and on reaction-field

(16) Brandrup, J.; Immergut, E. H. *Polymer Handbook*, 3rd ed.; Wiley Interscience: New York, 1988; pp V15–V16.
(17) Reilly, P. D.; Skinner, J. L. *Phys. Rev. Lett.* **1993**, *25*, 4257–4260.
(18) (a) Shalev, E.; Ben-Horin, N.; Even, U.; Jortner, J. *J. Chem. Phys.* **1991**, *95*, 3147–3166. (b) Shalev, E.; Ben-Horin, N.; Jortner, J. *J. Chem. Phys.* **1992**, *96*, 1848–1853. (c) Heidenreich, A.; Bahatt, D.; Ben-Horin, N.; Even, U.; Jortnerr, J. *J. Chem. Phys.* **1994**, *100*, 6300–6308.
(19) Nicol, M. F. *Appl. Spectr. Rev.* **1974**, *8*, 183–227.
(20) Brady, J. E.; Carr, P. W. *J. Phys. Chem.* **1985**, *89*, 5759–5766.
(21) Reichardt, C. *Solvents and Solvent Effects in Organic Chemistry*, 2nd ed.; VCH Publ.: Weinheim, 1988.
(22) Ghoneim, N.; Rohner, Y.; Suppan, P. *Faraday Discuss. Chem. Soc.* **1988**, *86*, 295–308.
(23) Ågren, H.; Mikkelsen, K. V. *J. Mol. Struct. (Theochem)* **1991**, *234*, 425–467.
(24) Bayliss, N. S.; McRae, E. G. *J. Phys. Chem.* **1954**, *58*, 1002–1006.
(25) McRae, E. G. *J. Phys. Chem.* **1957**, *61*, 562–572.

techniques,[37] treating the solvent as a continuum of known dielectric constant and polarizability.[2,19-22,28-31,37] These methods have provided general guidelines for the correlation of solvent shifts in liquids with the dielectric properties of the medium and have had considerable success.[2a,3,4,19-22,29-31] However, they are unable to provide detailed atomic-level information about the solvation process and cannot explain the significant exceptions that occur in certain solvents or with certain solutes.[2a,19,20] Finally, it must be stressed that such methods usually cannot establish an absolute scale for the solvent shift.[20]

With increased computational power more elaborate techniques have been developed and used. It has become customary to model the first (and sometimes also the second) solvation shell of a chromophore in a detailed manner, either using classical simulation methods[32,33] or quantum mechanical supermolecule approaches.[23,34-36] The coupling of this "exact" modeling of the first solvation shell with a reaction field method for the solvent molecules beyond has provided important insights in the nature of the microscopic interactions contributing to the solvent shift. It thus appears that, even in the case that strong specific interactions exist (e.g., through hydrogen bonding), a significant part of the shift is due to *nonspecific interactions*, such as dispersion and polarization interactions.[33c] Furthermore, even in the case of strong specific interactions, most of the solvent shift can be attributed to the first solvation shell. Contributions of solvent molecules located further away from the solute are usually of minor importance,[33c] unless the solute is charged or there is a very large difference in charge separation between the ground and excited states.

Supermolecule approaches such as those of Mikkelsen and co-workers[23,35,36] or of Luzhkov and Warshel[34] are very valuable, but they are still today computationally intractable when it comes to modeling large systems with significant long-range interactions. Simpler methods based on classical simulation (to provide solute–solvent structures) and many-body reaction-field techniques[37] appear to hold much promise.[32,33] Furthermore, in the absence of strong long-range interactions it is possible to obtain good estimates of the spectral shifts just from classical methods alone.[32] This is usually done by invoking the classical Franck–Condon principle in the case of electronic absorption spectra, provided a good parametrization of pair potentials for the excited state is available.

The arsenal of methods for calculating solvent shifts has recently been enlarged by a new semiempirical method from the group of Jortner,[18] originally developed for calculations of *dispersive* shifts in van der Waals clusters. This method is a generalization of the old Longuet-Higgins/Pople model (LHP) of dispersive solvent shifts[26] and is in principle more attractive than older approaches, since it accounts for the finite size of the chromophore by going beyond a point-dipole expansion of the transition moment. We will discuss this method in more detail in section V and Appendix A.

II.2. Modeling of Inhomogeneous Broadening of Absorption Spectra. In contrast to a liquid, in which the environment of each chromophore is rapidly changing with time, chromophores in low temperature solids find themselves in distinct environments that change very slowly with time. The absorption band of a chromophore in a solid tends to be "inhomogeneously" broadened as a result of the considerable variation of local environments.[6,38,39] The broadening is particularly large in amorphous solids, the width of the inhomogeneous band being much larger than the width of the individual single-molecule absorption line.[6,38,39] Furthermore, while single-molecule (zero-phonon) lines are Lorentzian, their convolution often has a broad Gaussian shape in glassy matrices.[6,12,13] The initial attempts to obtain the full transition line shape in a solid have been reviewed by Stoneham in his seminal article.[38] In order to obtain the spectrum, it is necessary to use a statistical approach. Several alternatives have been developed to date. It is possible to use approximate stochastic methods, such as that of Kubo,[38,40] liquid state radial distribution functions for liquid or glassy solvents,[23,41] lattice models (especially in crystalline materials),[42] or computer-generated pair distribution functions for specific model systems.[43] None of these methods is readily applicable to an amorphous glassy polymer. The procedure adopted in this study is to generate a reasonably large number of uncorrelated structures of a polymer-chromophore system and to try to deduce from this collection the properties of a statistical ensemble. This is a technique that has been used with success in the past in a large number of calculations involving atomistically-detailed polymer modeling.[44-46] Each structure considered in detail is identified with a "site" in the real system, and its transition frequency is estimated. Of course, different sites may accidentally exhibit similar frequencies.

III. Description of the System

III.1. Introductory Remarks. Our initial goal was to study a system, in which the simplest possible interactions are active. The obvious choice is a nonpolar chromophore in a nonpolar, *completely amorphous* polymer matrix. We have chosen atactic polypropylene as the matrix (Figure 1a), since it is a nonpolar polymer that has virtually no crystallinity in the glassy state.[47] The choice of a proper chromophore is more difficult. It must be a molecule with interesting photochemical properties and a reasonably small size for computational expedience (large complicated chromophores, such as porphyrins and chlorin, are

(26) Longuet-Higgins, H. C.; Pople, J. A. *J. Chem. Phys.* **1957**, *27*, 192–194.
(27) Marcus, R. A. *J. Chem. Phys.* **1965**, *43*, 1261–1274.
(28) Bauer, M. E.; Nicol, M. *J. Chem. Phys.* **1966**, *44*, 3337–3343.
(29) (a) Liptay, W. *Z. Naturforsch.* **1965**, *20a*, 1441–1471. (b) Liptay, W. *Angew. Chem., Int. Ed. Engl.* **1969**, *8*, 177–188. (c) Liptay, W.; Walz, G. *Z. Naturforsch.* **1971**, *26a*, 2007–2019.
(30) Brunschwig, B. S.; Ehrenson, S.; Sutin, N. *J. Phys. Chem.* **1987**, *91*, 4714–4723.
(31) Kamlet, M. J.; Abboud, J. L.; Taft, R. W. *Prog. Phys. Org. Chem.* **1980**, *13*, 485–630.
(32) Debolt, S. E.; Kollman, P. A. *J. Am. Chem. Soc.* **1990**, *112*, 7515–7524.
(33) (a) Zeng, J.; Craw, J. S.; Hush, N. S.; Reimers, J. R. *J. Chem. Phys.* **1993**, *99*, 1482–1495. (b) Zeng, J.; Hush, N. S.; Reimers, J. R. *J. Chem. Phys.* **1993**, *99*, 1496–1507. (c) Zeng, J.; Hush, N. S.; Reimers, J. R. *J. Chem. Phys.* **1993**, *99*, 1508–1521.
(34) Luzhkov, V.; Warshel, A. *J. Am. Chem. Soc.* **1991**, *113*, 4491–4499.
(35) Mikkelsen, K. V.; Ågren, H.; Jensen, H. J. Aa.; Helgaker, T. *J. Chem. Phys.* **1988**, *89*, 3086–3095.
(36) Ågren, H.; Knuts, S.; Mikkelsen, K. V.; Jensen, H. J. Aa. *Chem. Phys.* **1992**, *159*, 211–225.
(37) (a) Onsager, L. *J. Am. Chem. Soc.* **1936**, *58*, 1486–1493. (b) Kirkwood, J. G. *J. Chem. Phys.* **1934**, *2*, 351–361. (c) Kirkwood, J. G. *J. Chem. Phys.* **1939**, *7*, 911–919. (d) Block, H.; Walker, S. M. *Chem. Phys. Lett.* **1973**, *19*, 363–364.
(38) Stoneham, A. M. *Rev. Mod. Phys.* **1969**, *41*, 82–108.
(39) Rebane, K. K.; Rebane, L. A. in ref 8, pp 17–77.
(40) Kubo, R. *Adv. Chem. Phys.* **1969**, *15*, 101–127.
(41) Saven, J. G.; Skinner, J. L. *J. Chem. Phys.* **1993**, *99*, 4391–4402.
(42) Orth, D. L.; Skinner, J. L. *J. Phys. Chem.* **1994**, *98*, 7342–7349.
(43) (a) Laird, B. B.; Skinner, J. L. *J. Chem. Phys.* **1989**, *90*, 3274–3281. (b) Sevian, H. M.; Skinner, J. L. *Theor. Chim. Acta* **1992**, *82*, 29–46.
(44) Theodorou, D. N.; Suter, U. W. *Macromolecules* **1985**, *18*, 1467–1478.
(45) (a) Theodorou, D. N.; Suter, U. W. *Macromolecules* **1986**, *19*, 379–387. (b) Hutnik, M.; Argon, A. A.; Suter, U. W. *Macromolecules* **1991**, *24*, 5970–5979. (c) Rutledge, G. C.; Suter, U. W. *Polymer* **1991**, *32*, 2179–2189.
(46) (a) Gusev, A. A.; Suter, U. W. *Phys. Rev. A* **1991**, *43*, 6488–6494. (b) Gusev, A. A.; Suter, U. W. *J. Chem. Phys.* **1993**, *99*, 2228–2234.
(47) *Physical Structure of the Amorphous State*; Allen, G., Petrie, S. E. B., Eds.; Marcel Dekker: New York, 1977.

ruled out in this way). In the absence of a previous atomistic investigation, precise knowledge of the force field and the geometric and electronic structure of the ground and the excited state was considered a basic requirement for this project. Relatively large nonpolar chromophores, such as cata-condensed or peri-condensed aromatic hydrocarbons (e.g., tetracene, pentacene, perylene) have been used extensively in hole-burning studies of glasses.[3,6,8,9] Even though such molecules can be studied by classical simulation methods, it is difficult to perform high-level ab initio calculations on their excited states. Therefore, we have chosen *s*-tetrazine (Figure 1b), a much simpler and smaller nonpolar molecule, which undergoes a photochemical decomposition reaction in hole-burning spectroscopy in solids. In the course of this investigation it became obvious that a larger chromophore could have been used with equal success in this nonpolar polymer matrix (see section VI). However, this was not obvious to us in the beginning.

III.2. Classical Force Field for Polypropylene. The polymer is modeled with a classical force field. We have used Biosym's DISCOVER molecular simulation program[48] to create the polymer structures and decided to use the *pcff91* force field[49] which reproduces room-temperature thermodynamic and mechanical properties of several nonpolar polymers in a satisfactory way.[50] *pcff91* is a complex, second-generation force field, composed of many terms that attempt to accurately describe intramolecular (mostly bonded) interactions within a complex molecule. The nonbonded interactions between pairs of atoms i and j are given by the sum of an electrostatic, an exchange-repulsion term, and a dispersion term

$$U_{ij}^{nb} = \frac{q_i q_j}{r_{ij}} + \epsilon_{ij}\left[2\left(\frac{r_{ij}^{min}}{r_{ij}}\right)^9 - 3\left(\frac{r_{ij}^{min}}{r_{ij}}\right)^6\right] \quad (1)$$

where the q_i's are partial charges located on atomic sites, r_{ij} is the interatomic distance between atoms i and j, ϵ_{ij} is a the depth of the potential well of the interaction, and r_{ij}^{min} is the position of the bottom of the potential well. The (fictitious) partial charges on carbon and hydrogen atoms are grouped in such a way that ethyl, methylene, and methine groups are each neutral overall. The partial charge on hydrogen atoms is +0.053e, leading to a value for the dipole moment of the C−H bond of 0.3 D, in good agreement with published values.[51a] The density of the polymer at temperatures in the range of 10−30 K is roughly 0.93−0.95 g/cm^3, obtained by extrapolation from a specific volume vs temperature plot provided by Armeniadis and Baer.[52] The built-in *pcff91* r_i^{min} values of carbon and hydrogen were reduced by 3% to reproduce the density of polypropylene in the range of 10−30 K.[50] It was found that the modified force field reproduces the density of the glass well at low temperatures, while the original force field produces structures, the density of which is 5−8% lower (results not shown here).

III.3. Quantum Calculations on s-Tetrazine. In order to make quantitatively appropriate parameters available to the classical molecular simulation, we performed a series of ab initio computations on the ground state and the first excited state (S_0,S_1) of *s*-tetrazine. This appeared necessary since, although the azabenzenes have been extensively studied at the experimental[53−57] and at the theoretical[58−64] level, some of the excited state properties of *s*-tetrazine that have been subject to debate in the experimental literature and basic issues, such as the geometry of the first excited state structure, are not fully resolved.[54−56] The results of our own detailed quantum chemical study on the ground- and first-excited-state properties of *s*-tetrazine are presented in a separate publication.[65]

From the ab initio computations we generated a force field and an electrostatic potential (ESP), from which a set of distributed monopoles centered on the atomic sites for the ground and the first excited state were derived. The force field information is actually required for the electronic ground state only in the present work and was generated using the CCSD-(T) variant of the coupled cluster method.[66] The computations were performed with a 6-311G(d,p) basis set using the program ACES II.[67] The optimized geometry of the ground and first electronic excited state, obtained at the CCSD(T) and the CASSCF/PT2 level (14 electrons in 14 active orbitals),[65] are provided in Table 1 for comparison with the classical force field discussed in the next section. The harmonic frequencies were computed from numerical differentiation of the analytical CCSD(T) gradients of the energy. All electrons were correlated in this calculation. The frequencies obtained are tabulated in Table 2 and are in very good agreement with experiment.

The electrostatic information is required for both electronic states and was computed using the MP2 method for the ground state and the single-excitation configuration interaction method (CIS; ref 68) for the excited state. Point charges on the atoms of *s*-tetrazine were generated from the electrostatic potential (ESP) by a least-squares fitting procedure and are presented in Table 3, together with the zz component of the traceless quadrupole moment tensor,[51b] which is a measure of the polarity of the molecule. The computation of the ESP as well as the fitting procedure for the charges are implemented in the Gaussian92 program.[69] The grid for the computation of the ESP was generated according to the method of Kollmann and co-

(48) DISCOVER User Guide, Versions, 2.9.0/3.1.0, Copyright 1993, Biosym Technologies Inc., San Diego, CA.
(49) Maple, J. R.; Hwang, M.-J.; Stockfisch, T. P.; Dinur, U.; Waldman, M.; Ewig, C. S.; Hagler, A. T. *J. Comput. Chem.* **1994**, *15*, 162−182.
(50) Gusev, A. A., personal communication.
(51) (a) Hopfinger, A. J. *Conformational Properties of Macromolecules*; Academic Press: London, 1973. (b) Gray, C. J.; Gubbins, K. E. *Theory of Molecular Fluids*; Clarendon Press: Oxford, 1984.
(52) Armeniadis, C. D.; Baer, C. In *Introduction to Polymer Science and Technology*; Kaufman, H. S., Falcetta, J. J., Eds.; John Wiley: New York, 1977.
(53) Sigworth, W. D.; Pace, E. L. *Spectr. Acta* **1971**, *27A*, 747−758.
(54) Smalley, R. E.; Wharton, L.; Levy, D. H.; Chandler, D. W. *J. Mol. Spectrosc.* **1977**, *66*, 375−88.
(55) Job, V. A.; Innes, K. K. *J. Mol. Spectrosc.* **1978**, *71*, 299−311.
(56) Innes, K. K.; Ross, I. G.; Moomaw, W. R. *J. Mol. Spectrosc.* **1988**, *132*, 492−544.
(57) Heitz, S.; Weidauer, D.; Hese, A. *J. Chem. Phys.* **1991**, *95*, 7952−7956.
(58) Mulder, F.; Van Dijk, G.; Huiszoon, C. *Mol. Phys.* **1979**, *38*, 577−603.
(59) Papadopoulos, M. G.; Waite, J. *J. Chem. Phys.* **1985**, 1435−1436.
(60) Lorite Villacreces, I.; Fernandez Gomez, M.; Lopez Gonzalez, J. J.; Cardenete Espinosa, A. *Spectr. Acta* **1987**, *43A*, 873−878.
(61) Scheiner, A. C.; Schaefer, H. F. *J. Chem. Phys.* **1987**, *87*, 3539−3556.
(62) Mó, O.; De Paz, J. L. G.; Yáñez, M. *J. Mol. Struct. (Theochem)* **1987**, *150*, 135−150.
(63) Prasad, R. S.; Rai, B. N. *Theor. Chim. Acta* **1990**, *77*, 343−357.
(64) Archibong, E. F.; Thakkar, A. J. *Mol. Phys.* **1994**, *81*, 557−567.
(65) Schütz, M.; Hutter, J.; Lüthi, H.-P. *J. Chem. Phys.*, submitted for publication.
(66) (a) Raghavachari, K.; Trucks, G. W.; Pople, J. A.; Head-Gordon, M. *Chem. Phys. Lett.* **1989**, *157*, 479−483. (b) Raghavachari, K.; Pople, J. A.; Replogle, E. S.; Head-Gordon, M. *J. Phys. Chem.* **1990**, *94*, 5579−5586. (c) Bartlett, R. J.; Watts, J. D.; Kucharski, S. A.; Noga, J. *Chem. Phys. Lett.* **1990**, *165*, 513−522.
(67) ACES II (Version 1.0), written by Stanton, J. F., Gauss, J., Watts, J. D., Lauderdale, W. J., and Bartlett, R. J., University of Florida, Gainesville.
(68) Foresman, J. B.; Head-Gordon, M.; Pople, J. A.; Frisch, M. J. *J. Phys. Chem.* **1992**, *96*, 135−149.
(69) Gaussian92/DFT, Revision F.4, written by Frisch, M. J., Trucks, G. W., Schlegel, H. B., Gill, P. M. W., Johnson, B. G., Wong, M. W., Foresman, J. B., Robb, M. A., Head-Gordon, M., Replogle, E. S., Gomperts, R., Andres, J. L., Raghavachari, K., Binkely, J. S., Gonzalez, C., Martin, R. L., Fox, D. J., Defrees, D. J., Baker, J., Stewart, J. J. P., and Pople, J. A., Gaussian Inc., Pittsburgh, PA, 1993.

Table 1. Geometry of the Ground State and the First Excited State of the *s*-Tetrazine Molecule[a]

Geometry of the Ground State

geometric parameter	*pcff91* force field	6-311G(d,p) CCSD(T)[65]	4s3p2d/3s2p ANO CASPT2[65]	exp[56]	exp[54]
C−C dist	2.50	2.530	2.527	2.534	2.538
C−N bond	1.33	1.345	1.339	1.340_5	1.338
N−N bond	1.30	1.332	1.326	1.326	1.334
C−H bond	1.07	1.086	1.074	1.07_3	1.070
N−C−N angle	126.5	127.1	126.7	126.4	126.5
C−N−N angle	116.8	116.5	116.7	116.8	116.8

Geometry of the First Excited State

geometric parameter	ab initio CASPT2[65]	exp[56]	exp[54]
C−C dist	2.623	2.608	2.669
C−N bond	1.333_1	1.324	1.358
N−N bond	1.320_5	1.349	1.280
C−H bond	1.073	1.06_3	
N−C−N angle	121.5	123.2	118.5
C−N−N angle	119.3	118.4	120.8

[a] All bonds are in Å and all angles in deg.

workers[70] and of Chirlian et al.[71] In connection to the ESP calculation we should point out that, to date, only a limited number of quantum chemical methods have been adapted for the computation of observables for singlet open-shell states, such as the $^1B_{3u}$ excited state of *s*-tetrazine. The CIS method is one of those methods, but it only represents Hartree−Fock level of accuracy. From our detailed quantum chemical study[65] we know that the ESP is reproduced with at least semiquantitative accuracy (i.e., the difference for the ESPs of the ground and the excited state is properly represented). In fact, the largest error introduced in the treatment of the electrostatics is that these interactions are modeled on the basis of atomic point charges rather than on the basis of a continuous electron density (see also ref 33 for a discussion of a similar problem for pyrimidine).

III.4. Classical Force Field for *s*-Tetrazine and Comparison to Quantum Calculations. The ab initio calculations on the ground state of *s*-tetrazine described above were used to check if the *pcff91* force field provides an accurate description of *s*-tetrazine. The geometry of the molecule in vacuum was optimized using the *pcff91* force field (modified as described in section III.2) and compared to the ab initio results and to available literature values. The results are presented in Table 1. In addition, normal-mode analysis of the ground-state vibrations was performed, and the resulting harmonic vibrational frequencies were compared to those calculated from ab initio methods and experimental vibrational frequencies (Table 2). These two comparisons are important in that they establish that the *intramolecular* part of the *pcff91* force field for *s*-tetrazine adequately reproduces the equilibrium geometry and harmonic vibrational frequencies of the ground state. Therefore, the *pcff91* force field can be used with some confidence to examine the degree of intramolecular distortion of the ground state of the chromophore in the polymer glass. The *pcff91* partial charges on the C, N, and H atoms do not agree however with those obtained from the ab initio calculations described above. We have used the ab initio generated partial charges (Table 3) in this study.

Upon excitation, the *polarity* of *s*-tetrazine decreases (see Table 3), but its polarizability increases. Heitz et al.[57] found

Table 2. Harmonic Vibrational Frequencies of the Ground State of *s*-Tetrazine (cm^{-1})

mode no.	*pcff91* force field	6-311G(d,p)[65] CCSD(T)	exp[56]
1	250	228	254
2	407	257	335
3	561	637	640
4	655	741	736
5	758	772	801
6	914	896	883
7	923	908	929
8	1050	947	994
9	1062	1018	1009
10	1110	1088	1093
11	1249	1137	1104
12	1259	1212	1204
13	1365	1321	1290
14	1379	1456	1415
15	1445	1471	1448
16	1630	1558	1525
17	3111	3222	3010
18	3114	3223	3086

Table 3. Partial Charges on the Ground- and Excited-States of the *s*-Tetrazine Molecule (in Electron-Charge Units), and the *zz*-Component of the Traceless Quadrupole Moment Tensor[51b] (in D·Å units)

property	ground-state ab initio MP2 (6-311G**)	excited-state ab initio CIS/S1 (6-311G**)
C charge	+0.843	+0.512
N charge	−0.366	−0.267
H charge	−0.110	+0.023
Q_{zz}	+0.652	+0.171

experimentally that the polarizability increases by about 10−20% and becomes more anisotropic upon excitation. The electrostatic effect can be modeled classically using revised values for the partial charges on *s*-tetrazine for the excited state, provided by the ab initio computations. The increased excited-state polarizability is more difficult to model classically. In many solvent-shift studies involving polar chromophores the change in dispersion interactions is ignored because it is difficult to estimate and usually much smaller than the direct polarization interactions.[32−34] For the present system dispersion is expected to provide the dominant contribution to the spectral shift. Within the context of a classical force field an increase in polarizability can be modeled as an increased attractive coefficient for the 6−9 potential of the excited state relative to the ground state. The approximate method that we used to parametrize the excited state of *s*-tetrazine is based on van der Waals cluster data of *s*-tetrazine with rare-gas atoms in the vapor phase. In principle, one may try to fit values for ϵ and r^{min} for the C, N, and H atoms of the chromophore in the excited state to reproduce spectral shift data for clusters of tetrazine with rare-gas atoms. This has already been done successfully for 6−12 Lennard-Jones potentials in cluster calculations with chromophores involving only C and H atoms.[18c,72] However, in the present case we have two more unknown parameters to fit and a much smaller body of cluster data. We have opted to use a different method to obtain excited-state parameters for *s*-tetrazine.

Our approach is based on the idea of Kettley et al.,[73] who modified the old Longuet-Higgins/Pople (LHP) model[26] to

(70) (a) Singh, U. C.; Kollman, P. A. *J. Comput. Chem.* **1984**, *5*, 129−145. (b) Besler, B. H.; Merz, K. M.; Kollmann, P. A. *J. Comput. Chem.* **1990**, *11*, 431−439.

(71) Chirlian, L. E.; Francl, M. M. *J. Comput. Chem.* **1987**, *8*, 894−905.

(72) (a) Fried, L. E.; Mukamel, S. *J. Chem. Phys.* **1992**, *96*, 116−135. (b) Ben-Horin, N.; Even, U.; Jortner, J.; Leutwyler, S. *J. Chem. Phys.* **1992**, *97*, 5296−5315. (c) Troxler, T.; Leutwyler, S. *J. Chem. Phys.* **1993**, *99*, 4363−4378.

(73) Kettley, J. C.; Palmer, T. F.; Simons, J. P.; Amos, A. T. *Chem. Phys. Lett.* **1986**, *126*, 107−12.

Table 4. Properties of Rare-Gas Atoms and Their Dimers with *s*-Tetrazine Needed To Obtain the Transition Energy Δ_M from Eq 4

rare-gas	I_A (eV)	α_A (Å^3)	$h\,\delta\nu_A$ (cm^{-1})	R_{AM} (Å)	$10^3 f_{AM}$
He[a]	24.9	0.205	1.37	3.285	0.29
Ar[a,b]	15.76	1.64	23	3.44	2.05
Kr[b]	14.0	2.48	32	3.50[c]	2.87
Xe[b]	12.13	4.04	45	3.69[c]	3.47

[a] From ref 74. [b] From ref 75. [c] These distances are not provided in ref 75. They were assumed to be identical to the corresponding numbers for tetracene and perylene provided by Kettley et al.[73]

account for the polarizability assymetry and the finite size of the chromophore. We assume that a rare-gas atom A and a chromophore molecule M interact at a distance R_{AM} through a 6−9 Lennard-Jones potential

$$U_{AM}(R_{AM}) = \frac{B_{AM}}{R_{AM}^9} - \frac{C_{AM}}{R_{AM}^6} \approx \sum_{m\in M} \epsilon_{Am}\left[2\left(\frac{r_{Am}^{min}}{R_{Am}}\right)^9 - 3\left(\frac{r_{Am}^{min}}{R_{Am}}\right)^6\right] \quad (2)$$

where the parameters ϵ and r^{min} have already been defined in eq 1 and R_{Am} is the distance of atom m on the chromophore from the rare-gas atom, A. We also assume that the coefficient of the attractive term, C_{AM}, is determined from dispersion forces alone and that *upon excitation the repulsive part of this potential remains practically unchanged.* With these assumptions the model of Kettley et al.[73] predicts that the change in the dispersive coefficient, C, upon excitation is

$$\frac{C_{AM}^e}{C_{AM}^g} \simeq 1 + \frac{\Delta_M}{\mathcal{E}_0 + \mathcal{F}_0} \quad (3)$$

where $\mathcal{E}_0$ and $\mathcal{F}_0$ are average excitation potentials for the chromophore M and the rare-gas atom A, respectively, and Δ_M is an average transition energy for the chromophore. According to Kettley et al.,[73] Δ_M should not be set equal to the actual transition energy in vacuo because this leads to a gross overestimation of C_{AM}^e/C_{AM}^g. It is better to view Δ_M as an adjustable chromophore-specific parameter, which can be obtained from the following spectral shift equation for A−M complexes

$$\delta\nu_{A-M} = \frac{1}{4hR_{AM}^6}\alpha_A(\alpha_{xx}^M + \alpha_{yy}^M + 4\alpha_{zz}^M)\frac{I_A I_M}{(I_A + I_M)^2}\Delta_M = f_{AM}\Delta_M \quad (4)$$

where the I's are (tabulated) first ionization potentials, α_A is the ground-state polarizability of the rare-gas atom, and α_{ii}^M are the diagonal ground-state polarizability components for a *planar* chromophore. The red shift, $\delta\nu_{A-M}$, of the van der Waals complex and the equilibrium approach distance of the rare-gas atom to the center of the chromophore, R_{AM}, are spectroscopically determined quantities.[74,75] According to eq 4, a plot of $\delta\nu_{A-M}$ vs f_{AM} should be a straight line passing through the origin, with a slope equal to the required Δ_M. Such a plot is presented for *s*-tetrazine in Figure 2. The experimental results for polarizabilities, ionization potentials, $\delta\nu_{A-M}$, R_{AM}, and f_{AM}, on which this plot was based, are tabulated in Table 4. The least-squares straight line was forced to pass through the origin. The slope in Figure 2 is equal to 1.5 ± 0.15 eV. Application of eq 3, using the values $\mathcal{E}_0 = I_M = 9.72$ eV,[76] and $\mathcal{F}_0 = I_A \simeq$ 9.5 eV (average of values for CH, CH_2, and CH_3 groups[77])

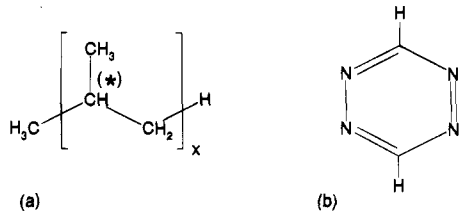

Figure 1. Chemical formulas for (a) polypropylene and (b) *s*-tetrazine.

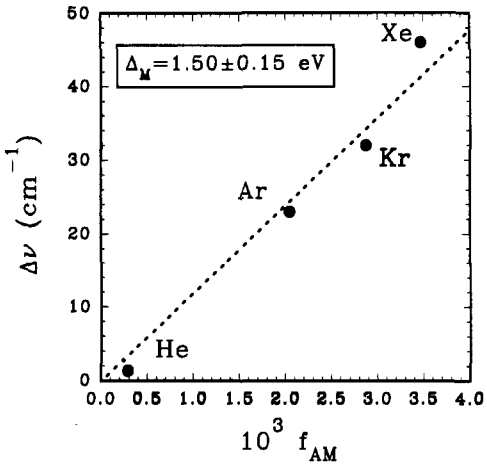

Figure 2. Determination of the factor Δ_M of eq 4 for *s*-tetrazine by plotting the experimental red shift $\delta\nu_{A-M}$ vs the function f_{AM}, where A is a rare-gas atom.

provides the estimate $C_{AM}^e/C_{AM}^g \simeq 0.08 \pm 0.02$. The uncertainty in this important ratio is thus substantial.

The *pcff91* force field requires *individual* ϵ and r^{min} values for the C, H, and N atoms of *s*-tetrazine in the excited state in order that the interactions of the excited state with the polymer matrix can be calculated. To obtain such values from the calculated ratio C_{AM}^e/C_{AM}^g, we must make additional approximations. First, we assume that the dispersive constants C_{AM} are obtained from additive contributions of individual atoms m on the chromophore [see eq 3] and that for all atoms m on M we have

$$\frac{C_{Am}^e}{C_{Am}^g} = \frac{C_{AM}^e}{C_{AM}^g}; \quad \forall\, m \in M \quad (5)$$

Second, we assume that the coefficients C_{Am} are connected to individual atomic parameters through a geometric mixing rule

$$C_{Am} = \sqrt{C_A C_m} \rightarrow \frac{C_m^e}{C_m^g} = \left(\frac{C_{Am}^e}{C_{Am}^g}\right)^2 \simeq 1.17; \quad \forall\, m \in M \quad (6)$$

Again it is assumed that upon excitation *the repulsive interactions are not affected.* Using the 6−9 form of the nonbonded interaction potential, we find that

$$\epsilon_m^e = 1.60\epsilon_m^g$$

$$r_m^{min,e} = 0.95 r_m^{min,g} \quad (7)$$

IV. Experimental Section

s-Tetrazine was synthesized as described by Spencer et al.[78] and kept in a small glass cell. A small piece of polypropylene (molecular weight ~ 20 000) was added into the glass cell at ambient temperature.

(74) Haynam, C. A.; Brumbaugh, D. V.; Levy, D. H. *J. Chem. Phys.* **1984**, *80*, 2256−2264.
(75) Weber, P. M.; Rice, S. M. *J. Chem. Phys.* **1988**, *88*, 6120−6133.
(76) Gleiter, R.; Schehlmann, V.; Spanget-Larsen, J.; Fischer, H.; Neugebauer, F. A. *J. Org. Chem.* **1988**, *53*, 5756−5762.
(77) *CRC Handbook of Chemistry and Physics, 67th ed.*; CRC Press: Florida, 1986−7.
(78) Spencer, G. H.; Cross, J. P. C.; Wiberg, K. B. *J. Chem. Phys.* **1961**, *35*, 1939−1945.

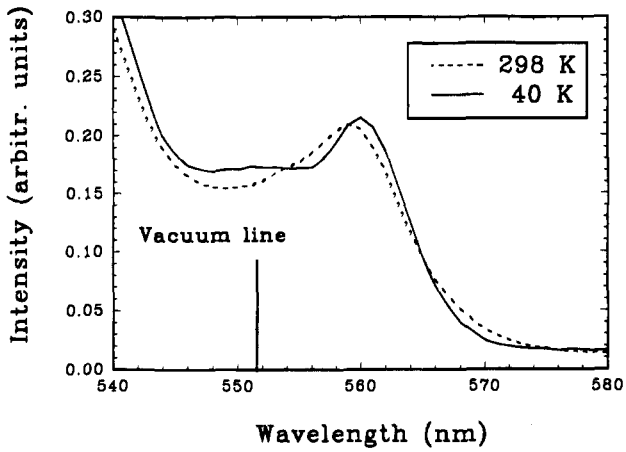

Figure 3. Absorption spectra of *s*-tetrazine in atactic polypropylene at room-temperature (dotted line) and 40 K (solid line). The part of the absorption spectrum between 540 and 580 nm is shown. The center of the $S_1 \leftarrow S_0$ band is at 560 nm.

The chromophore started diffusing into the polypropylene. After 48 h the chromophore-containing (red-colored) polymer was pressed between two glass plates, resulting in a thin film (thickness 200–300 μm) of sufficient optical quality (maximum absorbance of the $S_1 \leftarrow S_0$ band was 0.2). The chromophore concentration in the polymer was estimated to be approximately 10^{-2} mol/L, which corresponds to an interchromophore separation of 55 Å on average. Experiments, not reported here, show that the spectrum remains unchanged if the concentration is lowered. Absorption experiments were performed in a commercial spectrometer (Perkin-Elmer Lambda-9 series). An Oxford CF 1204 helium-flow cryostat provided cooling of the sample in the temperature range from room-temperature to 4 K. The inhomogeneously broadened spectrum does not change much below 100 K, so that the minimum temperature taken for the absorption measurements was 40 K. Spectra obtained at room-temperature and at 40 K are provided in Figure 3. The inhomogeneous band of the $S_1 \leftarrow S_0$ transition is not fully resolved (there is some overlap with the adjacent vibronic band), but the maximum can be clearly seen; it is shifted from the vacuum line (which occurs at 551.6 nm[54-57]) by approximately 8.5 nm (280 cm^{-1}). The width of the inhomogeneous band is estimated from Figure 3 to be 200–250 cm^{-1}.

V. Computational

V.1. Generation of Glassy Structures. Most of the structures created in this work contain a single polypropylene molecule of 103 repeat units (molecular weight = 4326) and a single *s*-tetrazine molecule in a cubic simulation cell of roughly 20 Å length. This minimum-image distance between chromophores is sufficient to ensure that chromophore–chromophore interactions are negligible (given that *s*-tetrazine is nonpolar) and very roughly corresponds to the experimental situation described in section IV. Since no significant long-range interactions are present in this system, the nonbonded interactions were truncated beyond 8.5 Å. The structures were generated in three different ways, in order to check the effect of the structure-generation method on the calculated polymer density and chromophore solvent shift. In method A we have generated an initial guess for the structure at 300 K and a density of 0.94 g/cm^3, using the method of Theodorou and Suter.[44] The energy of the structure was subsequently minimized at constant density using a combination of *NVT* molecular dynamics (with velocity-rescaling for temperature control) and the conjugate-gradient minimizer of the DISCOVER program on all internal degrees of freedom. The structure was finally quenched to 15 K, and *NpT* molecular dynamics (with velocity-rescaling for temperature control and the method of Berendsen et al.[79] for keeping the pressure constant) was run for roughly 100–200 ps, until the density and the various energy components of the structure had equilibrated. Method B is similar to method A, the main difference being that we have generated the structure at 300 K and the proper density for that temperature (roughly 0.85 g/cm^3, see ref 52) and have subsequently used temperature annealing of the structure to 15 K using six temperature steps (250, 200, 150, 100, 50, 15 K) with *NpT* molecular dynamics and an external cutoff-correction pressure of 1100 atm, corresponding to the 6–9 Lennard-Jones cutoff of 8.5 Å. In method C the initial guess was generated at 300 K and a low density (roughly 0.5 g/cm^3). The structure was subsequently compressed at 15 K with the external cutoff-correction pressure of 1100 atm. Methods B and C have given results comparable to method A, regarding both the final density and energy of the structure, and the eventually obtained solvent shift. We have subsequently used the simplest method, A, for most of the structures created for this project. Before accepting a structure in our "ensemble", we have tested not only energy and density equilibration, but also various structural features, such as the end-to-end distance of the chain, the pair distribution function for carbon atoms and the distribution of voids in the structure through a Voronoi tesselation. In Figure 4 we present an equilibrated glassy structure of tetrazine-containing polypropylene. This figure helps to illustrate the density of the packing in the solid phase and the relative sizes of the chromophore and the solvating groups of the polymer.

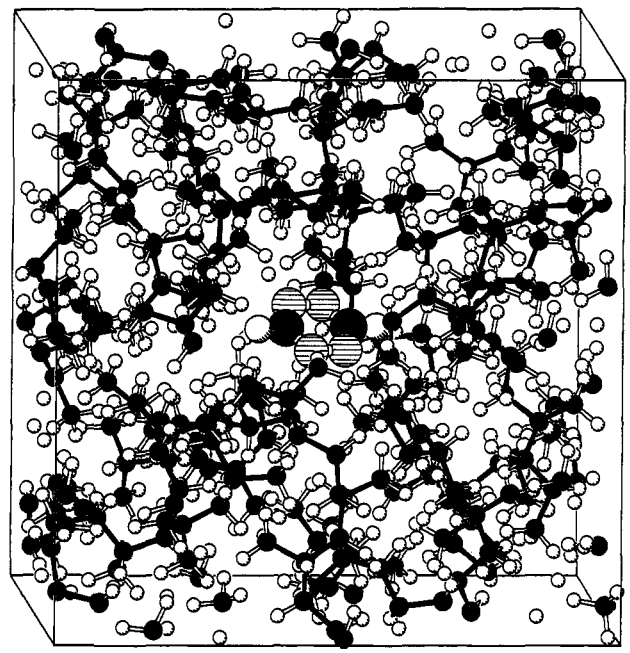

Figure 4. A glassy-polypropylene structure containing a single *s*-tetrazine molecule. Carbon atoms and carbon–carbon bonds are drawn black, hydrogens are white, and nitrogens are hatched. Atoms on the *s*-tetrazine are larger by a factor of 2 for better contrast.

Three "special" structures were additionally generated, all using method A. The first contained 210 repeat units of the polymer (molecular weight = 8840), the cube length being 24.5 Å and the cutoff-correction pressure 470 atm. This structure was used to investigate possible size and end-group-density effects. There was also a 20 Å structure containing *two* *s*-tetrazine molecules (positioned so that the distance of the two ring centers was approximately 10 Å) to check for possible effects of chromophore interactions on the spectral shift. Finally, a 20 Å structure was created with a large hard-spherical "hole" of 6 Å diameter, positioned at a distance of 6.5 Å from the center of the tetrazine ring. This structure was created to check if the presence of a cavity has any strong effect on the solvent shift, by introducing additional inhomogeneity in the structure.

V.2. Classical Molecular Dynamics and the Franck–Condon Principle. The solvent shift of *s*-tetrazine in polypropylene can be obtained using the vertical excitation idea inherent in the Franck–Condon principle. The computational procedure is similar to that of DeBolt and Kollman[32] or of Saven and Skinner.[41] Sufficiently long trajectories of the ground-state of the molecule in the polymer are generated using *NpT* molecular dynamics. The solvent shift can then be calculated assuming that upon excitation the geometry of the molecule remains unchanged, whereas the electron distribution instantaneously changes to that of the excited state. We can define three characteristic time scales here: (i) the time-scale for electron redistribution upon excitation, τ_{el}, (ii) the integration time step for our classical molecular dynamics that generates the trajectory, τ_{MD}, and (iii) the time scale for intramolecular geometry relaxation, τ_{geo}. Use of the Franck–Condon principle requires that

$$\tau_{el} \ll \tau_{MD} \ll \tau_{geo} \tag{8}$$

which is approximately true, since τ_{el} is generally of order 0.1–1 fs (as determined by the uncertainty principle), τ_{MD} is 0.5–1 fs, and τ_{geo} is considerably longer than the time for a molecular-bond vibration,[80] i.e., longer than 100 fs.

Molecular dynamics calculations were started at 15 K, from a fully equilibrated glassy structure (obtained as described in section V.1) at a cutoff-correction pressure of 1100 atm (470 atm for the larger structure), using a timestep of 0.5 fs and a nonbonded interaction cutoff of 8.5 Å for the 20 Å structures, and 11.5 Å for the larger structure. The temperature was controlled to within 0.5 K using a velocity-rescaling method,[79] and the pressure was controlled using the method of Berendsen et al.[79] After an initial period of 3 ps, which we allow for relaxation of the initial atomic velocities, "snapshots" of the system were collected and stored every 50 fs for 20–30 ps. This ground-state trajectory can be used to obtain the solvent shift upon excitation. One simply "reads" the classically-obtained ground-state trajectory and recalculates the *intermolecular* interaction energy between the chromophore and the solvating groups of the polymer, using the *excited-state force field* for the chromophore. The difference between the original (ground-state) and the excited-state intermolecular interaction energies provides a momentary solvent shift. Averaging of this "instantaneous" value over the entire trajectory provides the average solvent shift for a specific polymer structure. We have implemented this classical procedure using the empirically-generated excited-state force field of section III.4.

It must be emphasized here that *we are using molecular dynamics only in order to obtain localized trajectories of our system on the ground-state potential energy surface*, that is, to obtain an accurate measure for the local energy and density fluctuations. We believe that the structures that we obtained are reliable, to the extent that the force field employed is satisfactory. However, the actual dynamics of the trajectory may not be of great value for the following reasons:

(a) *NpT* molecular dynamics is seldom equivalent to the microcanonical (Newtonian) MD. Especially at this low temperature, at which the rate of energy dissipation is low, the dominant mode of motion of the system is the "breathing" motion that accompanies simulation-cell fluctuations.

(b) *NpT* MD creates artificial strain on molecular bonds, since it scales *all* coordinates by the instantaneous box-fluctuation ratio.

(c) It is questionable whether purely classical MD is relevant at these very low temperatures. The classical treatment of

(79) Berendsen, H. J. C.; Postma, J. P. M.; van Gunsteren, W. F.; DiNola, A.; Haak, J. R. *J. Chem. Phys.* **1984**, *81*, 3684–3690.

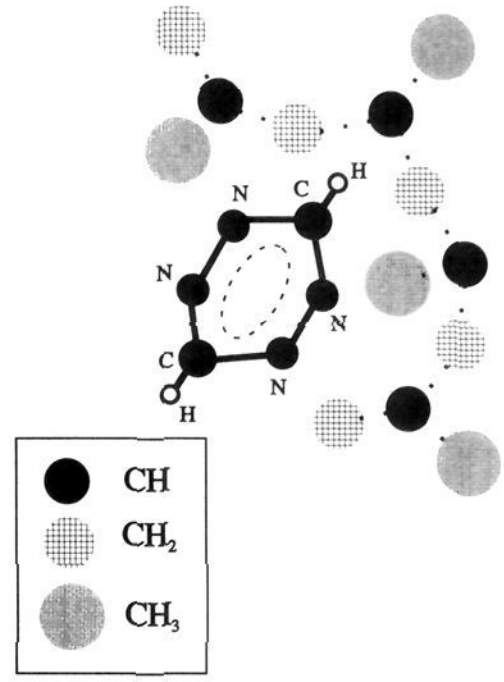

Figure 5. Schematic of the treatment of the polymeric solvating groups in the modified SBEJ approach as a mixture of independent spherical solvent "atoms".

degrees of freedom with characteristic frequencies ν, for which $h\nu/k_BT > 1$, is not justified. Strictly speaking, at $T = 1$ K, any phenomenon with characteristic time less than 100 ps cannot be correctly treated classically. At $T = 10$ K this limit drops to 10 ps, which is still large, given the time step of 0.5–1 fs that MD algorithms typically use.

V.3. A Semiempirical Method for the Dispersive Solvent Shift.[18] In a 1991 paper Shalev et al. (in what follows we will call this the SBEJ method) proposed a semiempirical theory for the spectral shift of the electronic origin of the $S_1 \leftarrow S_0$ transition of aromatic chromophores due to solvation with rare-gas atoms.[18a] This approach is also an extension of the Longuet-Higgins/Pople (LHP) formalism,[26] accounting for the finite size of the chromophore (compared to the chromophore-solvent distance). SBEJ employed a collection of monopoles, rather than a point-dipole, to represent the transition moments of the chromophore. According to the LHP derivation, these transition moments appear in the second-order terms of the dispersive chromophore solvent interactions. The spectral shifts for nonpolar chromophores in rare-gas solvent clusters can then be written in terms of sums and differences of electrostatic interactions of electric fields on the chromophore (due to the transition-monopole charge distributions of all single excitations from the S_0 and the S_1 reference states) and the corresponding induced point dipoles on the rare-gas atoms. The method is based on the assumptions that (a) no electron overlaps between the chromophore and the solvent atoms occur, that (b) the shift contains only dispersive contributions, and that (c) the contributions from individual solvent atoms are *additive*.

This semiempirical approach was applied to a series of different nonpolar aromatic hydrocarbons embedded in argon clusters of different sizes. SBEJ were able to predict and elucidate structural features of the solvent clusters, based on measured spectral shifts.[18] However, the original SBEJ formalism is restricted to $\pi^* \leftarrow \pi$ type $S_1 \leftarrow S_0$ electronic excitations, and only transition moments of $\pi^* \leftarrow \pi$ single excitations from the S_0 and S_1 states occur in the spectral-shift expression. In the context of this work we have adapted the SBEJ method for dispersive spectral shift calculations of *s*-tetrazine in matrices of atactic polypropylene. We are thus treating methyl, methylene, and methine groups on the polymer as a *mixture of rare-gas solvent atoms, the connectivity among those groups playing no role in the calculation* (see Figure 5). In addition, to enable the treatment of $\pi^* \leftarrow$ n type $S_1 \leftarrow S_0$ electronic excitations (such as that of *s*-tetrazine) we have extended the SBEJ theory to include the transition moments of all single excitations from

Table 5. Geometry of *s*-Tetrazine Dissolved in Polypropylene and in Vacuum[a]

geometric parameter	in polypropylene	in vacuum
C−N bond	1.33 ± 0.04	1.33 ± 0.02
N−N bond	1.31 ± 0.07	1.31 ± 0.01
N−C−N angle	125.4 ± 3.6	125.8 ± 2.5
C−N−N angle	116.7 ± 2.0	117.0 ± 2.6
C−N−N−C torsion angle	0.4 ± 12.9	0.0 ± 5.1
N−C−N−N torsion angle	−0.3 ± 12.4	0.0 ± 5.9

[a] All lengths are in Å and all angles in deg.

the S_0 and S_1 states in the expression for the solvent shift. The most important points of this extension and additional information on the testing of the method are summarized in Appendices A and B. Here, we state the final result of the modified SBEJ procedure for the solvent shift

$$\delta E_{tot} = \sum_{A} \delta E_A^{(i)} \tag{9}$$

where the index A extends over individual interacting solvent groups, and the index i goes over the three components of the solvent mixture (CH, CH_2, and CH_3). $\delta E_A^{(i)}$ is the shift-contribution from the interaction of the chromophore (M) with a single solvating group, given by

$$\delta E_A^{(i)} = \eta \alpha_i \mathcal{F}_i \sum_{m \in M} \sum_{n \in M} K_{mn} G_{mn}^A \tag{10}$$

where α_i is the ground-state "atomic" polarizability of solvating group i (see Appendix A), $\mathcal{F}_i$ is its ionization potential, G_{mn}^A is a geometric factor

$$G_{mn}^A = \frac{\mathbf{R}_{mA} \cdot \mathbf{R}_{nA}}{R_{mA}^3 R_{nA}^3} \tag{11}$$

depending on the relative distance and orientation of A and M, comprising two-atom (m-A-m) and three-atom (m-A-n) contributions, and K_{mn} is an electronic factor independent of the relative geometry of A and M, given in Appendix A. The empirical scaling parameter η is introduced to correct for the overestimation of the transition monopoles, due to the very simple molecular orbital scheme employed in the SBEJ approach (see Appendix A). η is both chromophore-dependent and solvent-dependent. The proper value to use in the polypropylene matrix should be obtained by fitting results of a *s*-tetrazine−methane cluster or of *s*-tetrazine in an alkane solid phase. Since such results are not available to date, we have used a scaling factor obtained by fitting the shift of the *s*-tetrazine-*krypton* dimer. We have chosen krypton because its polarizability is similar to that of the polymer (however its ionization potential is considerably higher—see Table 7). The value $\eta = 0.60$ was thus obtained and used in the polypropylene calculations.

The nicest feature of the SBEJ approach is the separation of electronic (K_{mn}) and geometric (G_{mn}^A) factors in eq 10. In addition, the effect of the solvent orbitals is lumped in with the polarizability and effective ionization potential, the latter of which occurs also in the electronic factor K_{mn} (see Appendix A). The separation enables the treatment of large solvent clusters,[18] and eventually also the treatment of large-molecule solvents (e.g., polymers), given certain conditions and approximations.

VI. Results and Discussion

VI.1. Is *s*-Tetrazine Distorted in the Polymer Matrix? Slight differences in the average geometry of the ground state in the glass may contribute to an apparent change in the excitation energy. Such changes might be brought about by strain due to the molecular packing in the solid phase. Molecular distortions (especially of torsion angles) can certainly be expected for large chromophores, and such a finding has already been reported for pentacene in *p-terphenyl* crystals[81a] and even dimethyl-*s*-tetrazine in a mixed-alcohol glass.[81b] To resolve this issue in the present case, we have generated trajectories of 10 ps length from two tetrazine-containing polymer structures and also a corresponding trajectory of tetrazine in vacuum. We have calculated the average geometry of the chromophore in vacuum and in the solid phase. Comparison for some characteristic geometric parameters is given in Table 5, where it is seen that the distortion of the ground state of this small chromophore in the glassy phase is negligible. On the basis of the very small differences observed for the ground state, it is not reasonable to assume that strain-related distortion affects the solvent shift in the polymer glass.

VI.2. Do Electrostatic Interactions Contribute to the Shift? A significant charge redistribution occurs in *s*-tetrazine upon excitation, as discussed above (see section III.3 and Table 3). However, this should not contribute strongly to the solvent shift, since the polymer medium is completely nonpolar. We have checked this assumption by calculating the shift obtained, with the assumption that the excited state is characterized by the same Lennard-Jones 6−9 parameters as the ground-state,

Table 6. Electrostatic and Dispersive Contributions to the Spectral Shift of the $S_1 \leftarrow S_0$ Band of *s*-Tetrazine in Atactic Polypropylene[a]

structure	$\Delta U_{el}^{0\to1}$	$\Delta U_{disp}^{0\to1}$ (clas.)	$\Delta U_{disp}^{0\to1}$ (SBEJ)	$\Delta U_{tot}^{0\to1}$ (clas.)	$\Delta U_{tot}^{0\to1}$ (SBEJ)
1	−6.7 (−0.02)	−309 (−0.88)	−293 (−0.84)	−316 (−0.90)	−300 (−0.86)
2	−16.1 (−0.05)	−345 (−0.99)	−400 (−1.14)	−361 (−1.03)	−416 (−1.19)
2-*NVT*[b]	−16.8 (−0.05)	−346 (−0.99)		−362 (−1.04)	
3	+0.7 (+0.00)	−376 (−1.08)	−472 (−1.35)	−375 (−1.07)	−471 (−1.35)
4	−3.2 (−0.01)	−307 (−0.88)	−309 (−0.88)	−310 (−0.89)	−312 (−0.89)
5[c]	+19.3 (+0.06)	−382 (−1.09)		−363 (−1.04)	
	+0.7 (+0.00)	−410 (−1.17)		−409 (−1.17)	
6	−0.7 (−0.00)	−413 (−1.18)	−460 (−1.31)	−414 (−1.18)	−461 (−1.32)
7	+19.3 (+0.06)	−372 (−1.06)	−467 (−1.33)	−353 (−1.01)	−448 (−1.28)
7-LONG[d]	+18.4 (+0.05)	−373 (−1.07)		−355 (−1.12)	
8	−15.1 (−0.04)	−352 (−1.01)	−379 (−1.08)	−367 (−1.05)	−394 (−1.13)
9	−4.9 (−0.01)	−361 (−1.03)	−375 (−1.07)	−366 (−1.05)	−380 (−1.08)
B[e]	−2.1 (−0.01)	−315 (−0.90)	−340 (−0.97)	−317 (−0.91)	−342 (−0.98)
H[f]	−2.1 (−0.01)	−420 (−1.20)		−422 (−1.21)	
av[g]	−0.9 ± 11.2	−364 ± 38	−388 ± 67	−364 ± 37	−392 ± 64

[a] Simulation-cube size = 20 ± 0.3 Å. Trajectories generated using *NpT* molecular dynamics. Numbers in cm^{-1} (kcal/mol in parentheses). [b] Trajectory generated using *NVT* molecular dynamics. [c] This structure contains *two* *s*-tetrazine molecules. Distance between ring-centers = 10 Å. [d] Numbers generated from long trajectory (total length 250 ps - configurations stored every 0.5 ps). [e] Structure B is larger. Simulation-cube size = 24.5 ± 0.2 Å. [f] Structure H contains a spherical "hole" of 6 Å diameter. Initial distance between hole-center and ring-center of the *s*-tetrazine molecule = 6.5 Å. [g] Averages and standard deviations from all available structures in cm^{-1}.

Table 7. Polarizabilities and Effective Ionization Potentials of the Solvating Groups of the Polymer[a]

solvating group	polarizability (Å^3)	ionization potential (eV)
Ar	1.64	15.76
Kr	2.48	14.0
CH_4	2.60	12.7
CH_3	2.23	11.5
CH_2	1.85	9.3
CH	1.65	7.8

[a] The corresponding numbers for argon, krypton, and methane are also included for comparison.

Table 8. Calculated and Experimental Spectral Shifts $\delta\nu$ for the $S_1 \leftarrow S_0$ ($\pi^* \leftarrow$ n) transition of *s*-Tetrazine-Ar_n ($n = 1-4$) Solvent Clusters[a,b]

n	isomer	ΔE	$\delta\nu$ (comp)	$\delta\nu$ (exp)[74]
1	$(1+0)$	−302	−23	−23
2	$(1+1)$	−603	−46	−46
	$(2+0)$	−577	−39	
3	$(3+0)_1$	−951	−46	−64
	$(3+0)_2$	−946	−68	
	$(2+1)$	−888	−63	
4	$(4+0)$	−1325	−73	−73
	$(3+1)_1$	−1266	−68	
	$(3+1)_2$	−1260	−92	
	$(2+2)_1$	−1211	−89	
	$(2+2)_2$	−1170	−79	
14		−5750	−338	

[a] Several distinct isomers are listed for a given cluster size, denoted with labels such as $(m+n)_i$, where m and n mean the number of Ar atoms on the two sides of the chromophore and i is an index denoting the ith local minimum found for such a chromophore-solvent configuration. Thus, $(m+0)$ are *single-sided* and $(m+n)$ with $m, n > 0$ *double-sided* clusters. The corresponding intermolecular binding energies ΔE, obtained from the model potential used in the simulated annealing procedure, are also compiled for each isomer. [b] All energies and spectral shift values are in cm^{-1}. Unit conversion: 1 kcal/mol = 350 cm^{-1}.

the only difference between the two states being the different charge distribution. For the purposes of this calculation, the charge distribution on *s*-tetrazine was modeled with partial charges located on the atoms, as given in Table 3. From the results of this calculation (not shown here) it was found that the contribution of the direct electrostatic interaction is extremely small, as expected, amounting to less than 3% of the experimentally observed shift (Figure 3). These results were not corrected through a reaction-field scheme,[33c,34] because of the very low polarity of the polymeric matrix and the chromophore, and since the contribution of direct monopole interactions is practically negligible anyway. However, such a calculation would be necessary if the matrix or the chromophore had strong dipole moments.[19,29,33c,34] A direct measure of the relative insignificance of direct monopole interactions in these systems is given in Table 6, where the electrostatic contribution to the spectral shift is listed in the second column for the runs described in the next section and can be directly compared to the dispersive contributions.

VI.3. The Dispersive Contribution to the Spectral Shift. As stated before, there are two alternative ways of modeling the dispersive spectral shift in our system. On the one hand, the modeling of the increased polarizability of the excited state of *s*-tetrazine can be empirically carried out within the context of the classical *pcff91* force field by adjusting the dispersive coefficients of the 6−9 Lennard-Jones potential. We have done this, as described in section III.4, and have calculated solvent shifts for a number of structures by assuming that the intermolecular excited-state force field can be obtained as a combination of the (ab initio) distributed monopoles for the excited state and the new Lennard-Jones parameters calculated in section III.4. These results are listed in Table 6.

An alternative way to calculate the dispersive contribution to the solvent shift of *s*-tetrazine in polypropylene is provided by the extended SBEJ approach described in section V.3 and Appendix A. The CH, CH_2 and CH_3 groups of the polymer chains are treated as *independent spherical solvent beads* at the exact locations of the original groups, interacting with the chromophore like rare-gas atoms. Our modified SBEJ procedure[82] requires as input the polarizabilities and ionization potentials of CH, CH_2, and CH_3 groups. These were obtained from molecular polarizabilities and ionization potentials of series of linear and branched alkanes[77] by assuming group-additivity. They are tabulated in Table 7. The SBEJ method also requires MO coefficients and overlap integrals (needed in the evaluation of the electronic factor K_{mn}; see Appendix A). These were obtained from STO-3G SCF minimal basis set calculations. The results of the SBEJ method for the solvent shifts are presented in Table 6 together with the results of the previous method.

The solvent-shift results of Table 6 are presented in a pictorial way in Figure 6. The result from each structure is drawn as a thin line into the relevant part of the experimental spectrum. The following general conclusions can be based on this figure.

(a) The two methods for the calculation of the dispersive spectral shift give comparable results. The spread of the shift values appears to be smaller in the case of the classical calculation (the difference between the smallest and the largest shift calculated is 110 cm^{-1} (Figure 6—top) vs 180 cm^{-1} from the SBEJ calculation (Figure 6—bottom)). These numbers may be compared to the experimental width of the $\pi^* \leftarrow$ n band, which is roughly 200−250 cm^{-1}. The comparison must be viewed with caution, since one cannot be certain of the exact experimental inhomogeneous broadening (the band is not well resolved, since it is convoluted with the adjacent vibronic band), and because of the small size of the ensemble of structures that we generated in this study.

(b) The average solvent shift calculated with both methods appears to be larger than experimentally observed (calculated $\simeq -360$ cm^{-1} for the classical method and $\simeq -390$ cm^{-1} from the SBEJ method vs experimental $\simeq -280$ cm^{-1}). In the case of the classical approach, this is probably due to the inaccurate and highly approximate calculation of the excited-state Lennard-Jones parameters (see section III.4). In the case of the SBEJ method, the scaling factor, η, used is a source of uncertainty. Using the krypton-dimer (M−Kr) data to scale the calculation does not guarantee good results for an alkane-like condensed phase. Ideally, the scaling should be made using results from solid-like large clusters (*s*-tetrazine in an alkane matrix) or at least from the methane-tetrazine dimer. Another source of discrepancy arises from our neglect of change in the exchange-repulsions upon excitation. This is probably a reasonable

(80) Heller, E. J. *Acc. Chem. Res.* **1981**, *14*, 368−375.
(81) (a) Fleischhauer, H.-C.; Kryshi, C.; Wagner, B.; Kupka, H. *J. Chem. Phys.* **1992**, *97*, 1742−1749. (b) Pschierer, H.; Friedrich, J.; Falk, H.; Schmitzberger, W. *J. Phys. Chem.* **1993**, *97*, 6902−6906.
(82) Schütz, M. "Program POLYRED (Polymer Redshift Calculation)"; a copy of the program is available from the author upon request.
(83) (a) Stratt, R. M.; Adams, J. E. *J. Chem. Phys.* **1993**, *99*, 775−788; (b) Adams, J. E.; Stratt, R. M. *J. Chem. Phys.* **1993**, *99*, 789−799.
(84) Szabo, A.; Ostlund, N. S. *Modern Quantum Chemistry*; 1st ed. (rev.), McGraw-Hill: New York, 1989.
(85) (a) Mulder, F.; van Hemert, M.; Wormer, P. E. S.; van der Avoird, A. *Theor. Chim. Acta* **1977**, *46*, 39−62. (b) Mulder, F.; Huiszoon, C. *Mol. Phys.* **1977**, *34*, 1215−1235.
(86) Schütz, M.; Wülfert, S. "Program MOMO (Monte Carlo program for Molecular Clusters)"; a copy of the program is available from the authors upon request.

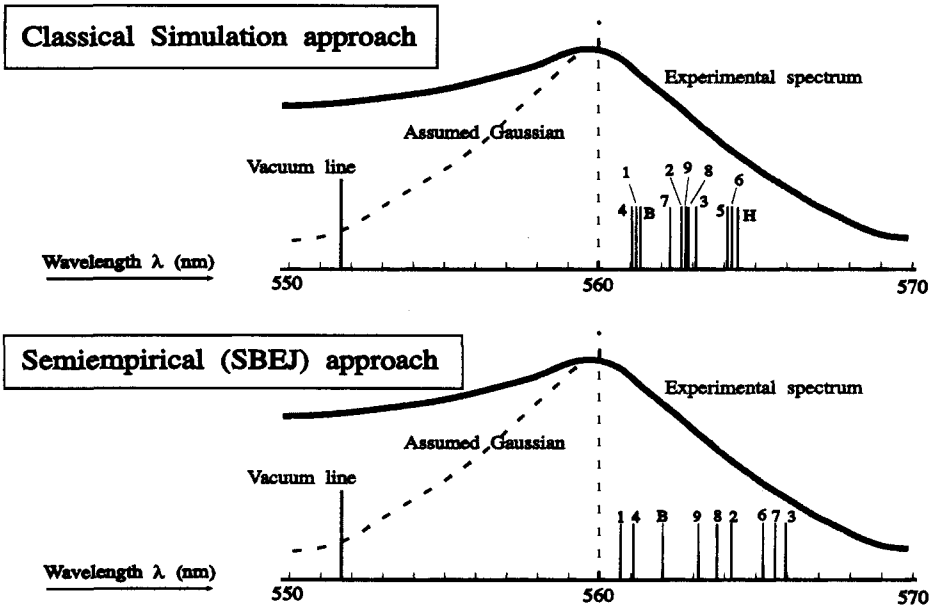

Figure 6. Absorption averages for the structures of Table 6 and the actual absorption spectrum of *s*-tetrazine in polypropylene.

assumption for clusters (although the interesting work of Stratt and Adams[83] implies that this is not always the case), but the interatomic distances in solids tend to be smaller, due to the high packing density. Whereas in a M−A vapor cluster the closest distance of approach of a rare-gas atom to a nitrogen or carbon atom of the tetrazine ring is 3.5−3.6 Å, in our glassy structures we typically find the first neighbors at a distance of 3.3−3.4 Å from nitrogen atoms. Increased repulsive intermolecular interactions in the excited state could be expected from the fact that the excited-state electronic structure is less localized. These repulsive interactions may produce a significant blue shift upon excitation and thus reduce the calculated total shift. It is noteworthy that the empirical parametrization of Heidenreich et al. for perylene-argon clusters leads to increased repulsions upon excitation.[18c] Similarly, Laird and Skinner use a model of increased repulsions upon excitation in their theory for the inhomogeneous broadening of absorption bands in glasses and claim that the changed repulsive interactions are responsible for the pressure-induced broadening of the homogeneous absorption lines.[43,5c] Theoretical calculations of Hartmannsgruber and Maier also imply that repulsive interactions might be important.[3e] Finally, Stratt and Adams[83] claim that repulsive interactions are necessary for correct interpretation of chromophore spectra for the whole range of solvent densities from clusters to solid phases.

(c) The solvent shift deduced from the larger structure falls within the range obtained with the smaller structures. Test-calculations with *NVT* molecular dynamics with a cutoff of 8.5 Å suggest that, while the cutoff-corrections to the intermolecular interactions of the polymer with the ground and the excited state of *s*-tetrazine are individually significant, they largely cancel each other out. On the basis of this—admittedly—limited evidence, we anticipate that there is no significant size-effect on the solvent-shift calculation.

(d) The length of the Molecular Dynamics trajectory used to evaluate the spectral shift appears to be sufficient, as evidenced by a single long-time calculation (structure 7-LONG in Table 6), in which we collected configurations every 0.5 ps for a total of 250 ps. This calculation demonstrates the lack of mobility in these low-temperature polymer glasses on the time-scale of nanoseconds.

(e) The presence of a 6 Å diameter "hole" in the structure, or the presence of a second chromophore at a distance of 10 Å, does not appear to have a significant impact on the solvent shift. This can be rationalized by the fact that the polarity of the polymer is very low, as is that of the chromophore. A "hole" in the structure might have a larger effect in a more polar polymer, since it introduces a local "vacuum" and makes the interactions in the vicinity of the solute more anisotropic. On the other hand, the close proximity of a dipolar chromophore should also have some visible effect. For the present system and on the basis of our scant evidence we must conclude that the breadth of the inhomogeneous band must be ascribed to local, nearest-neighbor packing fluctuations around the absorbing impurities. We will elaborate more on this point later.

(f) There is a good agreement between the shifts obtained with the two methods. Some discrepancy can be seen for structures 3 and 7, which give large shifts with the SBEJ method but only moderate shifts (smaller by 80−100 cm^{-1}) with the classical method. This disagreement is discussed below.

VI.4. Distance-Dependent Contributions to the Spectral Shift. In Figure 7 we plot the cumulative dispersive spectral shift as a function of distance from the center of the chromophore (summed over all solvent groups located within the indicated distance), obtained by the SBEJ method for four different structures. Although the plateau values for the shift are quite different in the four cases, most of the spectral shift is due to interactions with the first solvation cell (distances from 3 to 6 Å). This result does not depend on the cutoff used for the interactions, as seen by the curve for the larger structure. The cumulative-shift curves appear to have a maximum, but this is probably a cutoff-related artifact.

We have ascertained that the magnitude of the spectral shift does not depend on the actual volume of the simulation cell, i.e., on the cube-density. To find the reason for different spectral shifts in the different structures we plot in Figure 8a the *intermolecular* pair distribution functions $g_{C-N}(r)$ for the structures of Figure 7. The magnitude of the dispersive shift is obviously related to the density of polarizable matter in the first solvation cell around the chromophore: tightly packed solvent cages provide larger spectral shifts. By looking at the first-neighbor-peaks in Figure 8a, we observe that structure **6**, which gives the largest shift, exhibits a tighter packing around the chromophore than do structures **1** or **2**. Figure 8b clarifies this point further. Here we plot the number of neighboring matrix groups, $N_C(r)$, to the tetrazine ring as a function of the distance, r, from the center of the ring. $N_C(r)$ is obtained by integrating

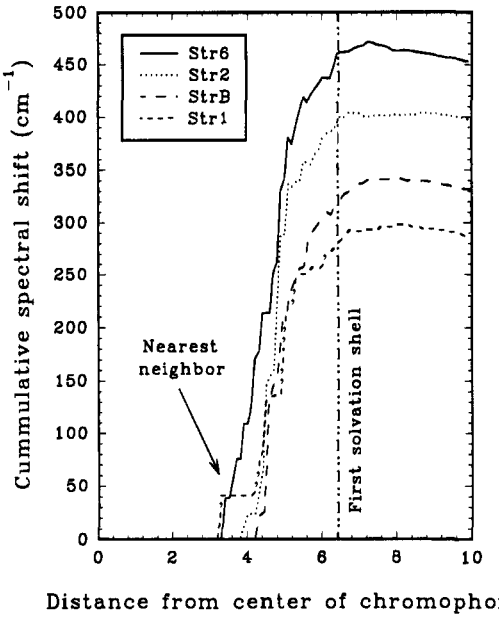

Figure 7. Cumulative (sum of all contributions from solvating groups within a given distance from the center of the chromophore) spectral shift (in cm^{-1}) as a function of the distance of the solvating groups from the center of the chromophore (in Å) for structures **6** (solid line), **2** (dotted line), B (long-dashed line), and **1** (short-dashed line).

the pair distribution function

$$N_C(r) = \frac{N_C^{tot}}{L^3} \int_0^r 4\pi x^2 g_{C-N}(x)\, dx \qquad (12)$$

where N_C^{tot} is the total number of carbon atoms in a simulation cube of edge-length L. The amplitudes of this function rank as Str6 > Str2 > StrB > Str1 in the range plotted, the same trend as in the shifts obtained in these structures. Interestingly, the chromophore in structure B has a larger number of neighbors beyond a distance of 6 Å but fewer neighbors than the chromophore in structure **2** in the region 3.5 Å < r < 5.5 Å. It thus appears that the first solvation shell of the chromophore determines most of the dispersive shift and that packing peculiarities play an extremely important role. This result serves to underline the difference between liquid and solid solvents. In the solid phase every chromophore site is "special" in a way, since the local packing and relative orientation of interacting solvent groups is different from site to site and cannot relax during the lifetime of the excited state.

The previously-mentioned difference in the predictions of the two models for structures **3** and **7** can also be understood through local-packing arguments. In Figure 9 we plot $N_C(r)/r^3$ for structures **3**, **6**, and **7**. This function tends to a constant (equal to $4\pi\varrho/3$ with ϱ the number density of solvating groups in the cube) when the pair distribution function goes to unity. From Figure 9 we see that *s*-tetrazine has more neighbors in the range 3.3 Å < r < 3.8 Å in structure **3**, while in the range 3.8 Å < r < 4.5 Å in structure **6** is more dense. The chromophore-solvent interactions in the SBEJ model contain three-body contributions and decay as R^{-4} for short distances between a solvent particle and the center of the chromophore (see eq 11), while at larger distances they switch to a "proper" R^{-6} dependence.[18] In contrast, the classical force field comprises a two-body, R^{-6} power-law for the dispersive interaction for all distances, which may not be suitable for short distances from π-electron rings. Hence, the SBEJ calculation is much more sensitive to the immediate environment of the chromophore. This is also the reason that the SBEJ model predicts a broader inhomogeneous absorption band, which is closer to the experimental result.

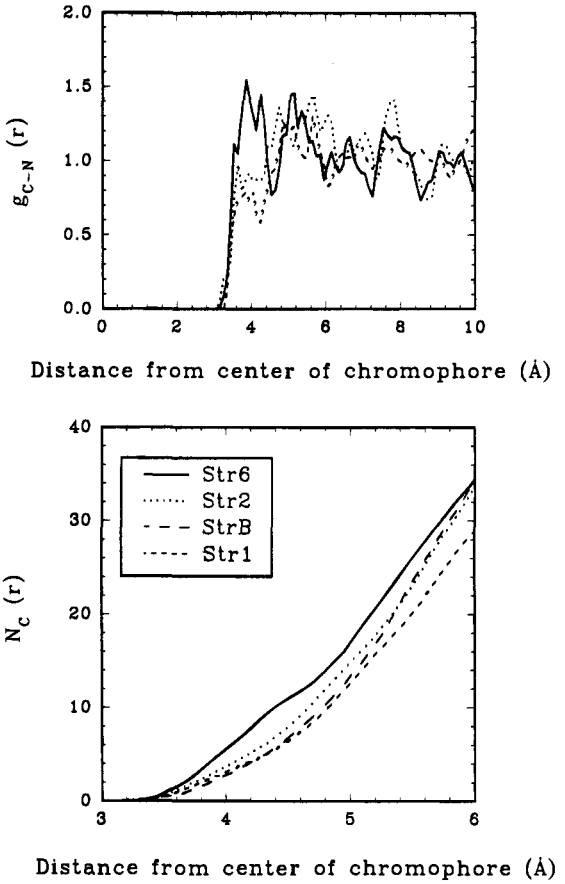

Figure 8. (a) Carbon–nitrogen pair distribution functions for structures **1**, **2**, and **6** as functions of distance in Å. Line-types as in Figure 7. (b) Integrated number of neighboring solvating groups of the polymer, $N_C(r)$, as a function of distance from the center of the chromophore for structures **1**, **2**, B, and **6**. Line-types as in Figure 7.

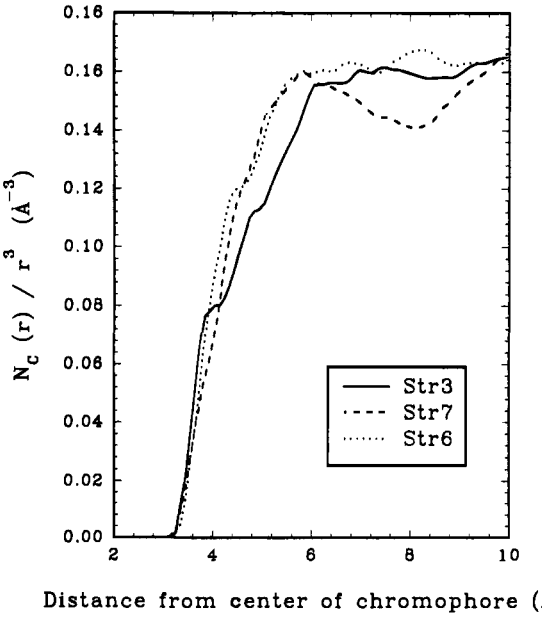

Figure 9. Integrated number of neighboring solvating groups of the polymer, $N_C(r)$, divided by r^3, as a function of distance r from the center of the chromophore for structures **3** (solid line), **6** (dotted line), and **7** (short-dashed line).

VII. Conclusions

We have carried out an experimental and computational investigation of the position and the width of the inhomoge-

neously-broadened band of the $^1B_{3u} \leftarrow {}^1A_g$ ($\pi^* \leftarrow$ n) transition of *s*-tetrazine in atactic polypropylene at low temperatures. Polymeric glassy structures containing the chromophore have been atomistically simulated and analyzed. We have found that the ground state of *s*-tetrazine is not significantly distorted in the solid phase and that the direct electrostatic (point-monopole) interactions contribute very little to the red spectral shift observed experimentally. Most of the shift is due to dispersion interactions that have been successfully modeled in two different ways: A systematic parametrization of the excited-state intermolecular potential of *s*-tetrazine allows the calculation of the spectral shift classically, using the Franck–Condon principle; in addition, the semiempirical method of Shalev et al.,[18] originally developed for rare-gas-solvent clusters containing chromophores undergoing $\pi^* \leftarrow \pi$ transitions, was generalized to chromophores undergoing $\pi^* \leftarrow$ n transitions and applied to a condensed polymeric phase for the first time. Both methods successfully predict the magnitude of the shift and provide a quantitative measure of the inhomogeneous broadening observed for this transition. An analysis of the energetic contributions to the dispersive shift revealed that the magnitude of the shift is almost completely determined by the first solvation shell of the chromophore, as already surmised in the literature.[3,5,33] Local packing in the solvent cage around the chromophore is of utmost significance. Whether this remains true in systems in which longer-range interactions are active is unclear at this point, although such a conclusion is implied by the work of Zeng et al.[33c] on solvent shifts of pyrimidine in water.

Our study of the inhomogeneously broadened band suggests that the width of the band is determined by the convoluted effect of packing and the dominant intermolecular interactions. We anticipate that systems in which additional interactions are active (e.g., induction effects in matrices with large permanent dipole moments or hydrogen bonding) could exhibit broader inhomogeneous bands, assuming that the variances of the shift-contributions from the different interactions are roughly additive. Existing experimental results appear to confirm this statement.[2b]

The results of the present work show that the combination of ab initio methods, semiempirical methods, and classical molecular dynamics is a valuable tool in the study of the interactions of chromophores with glassy solvents. As is common with such feasibility studies, possible extensions of this work are both numerous and fundamentally important. One can immediately think of at least three further avenues to explore.

(a) By adapting existing semiclassical approaches,[18c,41,72] one can obtain the individual molecule (microcanonical) absorption line shape. This provides valuable dynamic information. The ratio of the homogeneous to the inhomogeneous line width is of primary concern for hole-burning applications.[6,9,14] In particular, the evolution of the homogeneous line shape with time and with temperature may provide insights into potential spectral diffusion[13] and the processes that cause it.

(b) The extension of these calculations to other nonpolar chromophores, such as perylene, tetracene, and pentacene, for which a large body of spectroscopic data in the vacuum and in polymers exists, would be very valuable. Such an extension is certainly feasible, given that a precise characterization of the excited state of the chromophore is not critical in nonpolar matrices.

(c) It would be interesting to treat chromophores with permanent dipole moments in a nonpolar matrix by supplementing the SBEJ formalism with terms for inductive interactions.

The most interesting systems from the application point of view[3,4,6,8,14] are chromophores in highly polar matrices containing large permanent dipole moments or hydrogen-bonding moieties, such as poly(methyl methacrylate) and poly(vinyl butyral). The detailed atomistic treatment of such systems is considerably more difficult, since the significant induction effects of the polymer on the chromophore must be properly accounted for.

Acknowledgment. This work was supported by the Cray Research, Inc. University Research and Development Grant Program. E.L. would like to acknowledge useful discussions with Dr. A. A. Gusev of the Institute for Polymers, ETH, on the subject of choosing the proper potential force field for the polymer. We would also like to thank Mr. Guido Grassi of the Department of Physical Chemistry for the synthesis of *s*-tetrazine.

Appendix A: Modification of the SBEJ Theory for Spectral Shifts

In the framework of the Rayleigh–Schrödinger perturbation theory, the dispersive spectral shift δE_A of the I $\leftarrow$ 0 transition of a nonpolar chromophore M due to solvation by a rare-gas atom A can be written as the difference between two second-order terms

$$\delta E_A = \sum_{J\neq I}\sum_{P>0} \frac{|\langle\Psi_I\Phi_0|V|\Psi_J\Phi_P\rangle|^2}{E_I - (E_J + F_P)} - \sum_{J>0}\sum_{P>0} \frac{|\langle\Psi_0\Phi_0|V|\Psi_J\Phi_P\rangle|^2}{-(E_J + F_P)} \quad \text{(A1)}$$

Here, the unperturbed electronic states of the chromophore M and the rare-gas atom A are denoted by $|\Psi_J\rangle$ and $|\Phi_P\rangle$, respectively, and the corresponding excitation energies by E_J and F_P. The electronic ground state of the complex thus is $|\Psi_0\Phi_0\rangle$ with $E_0 = F_0 = 0$, while the relevant excited state is $|\Psi_I\Phi_0\rangle$ with excitation energy E_I. The intermolecular perturbation operator V describes the intermolecular interactions and comprises nucleus(M)–nucleus(A), nucleus(M)–electron(A), electron(M)–nucleus(A), and electron(M)–electron(A) contributions

$$V = \sum_{m\in M}\frac{Z_m Z_A}{R_{mA}} - \sum_{m\in M}\sum_{\alpha\in A}\frac{Z_m}{r_{m\alpha}} - \sum_{\mu\in M}\frac{Z_A}{r_{\mu A}} + \sum_{\mu\in M}\sum_{\alpha\in A}\frac{1}{r_{\mu\alpha}} \quad \text{(A2)}$$

where $\mathbf{r_m}$, $\mathbf{r_A}$ denote nuclear, and $\mathbf{r_\mu}$, $\mathbf{r_\alpha}$ electronic coordinates, respectively. In the following we will adhere to the common convention of using suffixes i,j,k,... for occupied, and a,b,c,... for virtual molecular orbitals on the chromophore. To distinguish between solute and solvent orbitals, occupied and virtual *atomic orbitals* centered on the rare-gas atoms are denoted by p,q,... and d,e,..., respectively. The electronic states of M and A are described in terms of singlet spin-adapted Slater determinants. The ground state $|\Psi_0\rangle$ of M corresponds to a single determinant with N occupied spin orbitals $\{\psi_j\omega\}$ (j = 1,..., $N/2$), and N unoccupied orbitals $\{\psi_b\omega\}$ ($b = N/2 + 1, \ldots, N$) (ω stands for α or β spin). The relevant excited state $|\Psi_I\rangle$ of M (for which the dispersive shift corresponding to the $\psi_a \leftarrow \psi_i$ excitation is calculated) is denoted by $|\Psi_i^a\rangle$. Since the last term of V (the *only* term that contributes to the sums of eq A1) is a two-electron operator coupling electrons of M with those on A, only single excitations from the reference functions $|\Psi_0\rangle$, $|\Psi_I\rangle$, and $|\Phi_0\rangle$ can contribute to the sums in eq A1. Therefore, only single excitations $|\Psi_j^b\rangle$, $|\Phi_p^d\rangle$ on M and A and double excitations of the type $|\Psi_{ij}^{ab}\rangle$ are relevant for the evaluation of the spectral shift. Because of the singlet spin restriction, open-

shell configurations are represented by the corresponding spin-adapted *configuration state functions* (CSFs).[84]

The matrix elements in eq A1 can be evaluated by application of the common Slater rules. Since the last term of V is a two-electron operator, coupling only one electron of $|\Psi_I\rangle$ with one of $|\Phi_P\rangle$, it acts as a one-electron operator on both $|\Psi_I\rangle$ and $|\Phi_P\rangle$. As a result, only *Coulomb integrals* appear in the expressions for the matrix elements:

$$\langle \Psi_0\Phi_0|V_{12}|\Psi_j^b\Phi_p^d\rangle = \int \psi_j(1)\left(\int \phi_p(2)\frac{1}{r_{12}}\phi_d(2)\,d\mathbf{r}_2\right)\psi_b(1)\,d\mathbf{r}_1 \doteq (jb|pd) \quad (A3)$$

For the matrix elements between the different CSFs one obtains after integration over spin space

$$\langle \Psi_0\Phi_0|V|\Psi_j^b\Phi_p^d\rangle = 2(jb|pd)$$

$$\langle \Psi_i^a\Phi_0|V|\Psi_0\Phi_p^d\rangle = 2(ia|pd)$$

$$\langle \Psi_i^a\Phi_0|V|\Psi_j^a\Phi_p^d\rangle = \sqrt{2}(ij|pd);\quad j\neq i$$

$$\langle \Psi_i^a\Phi_0|V|\Psi_i^b\Phi_p^d\rangle = \sqrt{2}(ab|pd);\quad b\neq a$$

$$\langle \Psi_i^a\Phi_0|V|{}^A\Psi_{ij}^{ab}\Phi_p^d\rangle = \sqrt{3}(jb|pd);\quad j\neq i;\quad b\neq a \quad (A4)$$

$$\langle \Psi_i^a\Phi_0|V|{}^B\Psi_{ij}^{ab}\Phi_p^d\rangle = 1(jb|pd);\quad j\neq i;\quad b\neq a$$

$$\langle \Psi_i^a\Phi_0|V|\Psi_{ii}^{ab}\Phi_p^d\rangle = \sqrt{2}(ib|pd);\quad b\neq a$$

$$\langle \Psi_i^a\Phi_0|V|\Psi_{ij}^{aa}\Phi_p^d\rangle = \sqrt{2}(ja|pd);\quad j\neq i$$

$$\langle \Psi_i^a\Phi_0|V|\Psi_{ii}^{aa}\Phi_p^d\rangle = 2(ia|pd)$$

Here, j,b denote occupied and virtual *spatial* MOs of M, whereas p,d signify occupied and virtual AOs centered on A. The prefactors 1, 2, $\sqrt{2}$, and $\sqrt{3}$ emanate from the spin coupling coefficients in the CSFs. Expanding linearly the MOs of M in the integral expression in terms of a set of basis functions $\{\mu,\nu,...\}$ gives

$$(jb|pd) = \sum_{m\in M}\sum_{\mu,\nu\in m} C_{j\mu}C_{b\nu}(\mu\nu|pd) \quad (A5)$$

In contrast to the original SBEJ formalism the basis set used to expand the MOs of M may comprise multiple distinct functions on the same atomic center m on M, rather than a single p_z function. However, to keep the formalism simple, three-center integrals are still disregarded in eq A5. The outer sum runs over all atomic centers m on M, while the inner double sum is only performed over pairs of basis functions μ,ν located on the same atomic site. This is a severe approximation, with the consequence that—due to deficiencies in the description of electron density located between atomic centers of M—terms from excitations involving σ or σ^* MOs are not properly accounted for. It is anticipated however that the dominant contributions to the spectral shift of the $\pi^* \leftarrow$ n transition come from $\pi^* \leftarrow \pi$ and $\pi^* \leftarrow$ n excitations. Contributions from remaining excitations appearing in the S_0 and S_1 stabilization energies should cancel out to a large extent. The integrals in eq A5 can be further simplified[18] by expanding the interaction operator $1/r_{12}$ in powers of $1/R_{mA}$ and truncating beyond the second-order term (R_{mA} is the distance between the center m of M and solvent atom A). Within this approximation the electron coordinates ξ_1 and ξ_2 in the two-electron integrals of eq A5 separate. One then obtains

$$\left\langle \mu(1)\phi_p(2)\left|\frac{1}{R_{mA}} - \frac{(\xi_1-\xi_2)\cdot\mathbf{R}_{mA}}{R_{mA}^3}\right|\nu(1)\phi_d(2)\right\rangle = \frac{\mathbf{R}_{mA}}{R_{mA}^3}\langle\phi_p(2)|\xi_2|\phi_d(2)\rangle\langle\mu(1)\nu(1)\rangle \doteq \frac{1}{\sqrt{2}}\frac{\mathbf{R}_{mA}}{R_{mA}^3}\cdot\boldsymbol{\mu}_{0P}S_{\mu\nu} \quad (A6)$$

Here, ξ_1 and ξ_2 denote electron coordinates relative to the centers m and A, respectively. $\boldsymbol{\mu}_{0P}$ is the transition dipole moment of the P $\leftarrow$ 0 ($\phi_d \leftarrow \phi_p$) excitation on A, and $S_{\mu\nu}$ is the overlap integral of the basis functions μ,ν, both located on the same center m.

Combining eqs A5 and A6 the matrix elements in eq A4 can be expressed in terms of the MO coefficients of M, $C_{j\mu}$, the overlap integrals, $S_{\mu\nu}$, and the transition dipole moments of A, $\boldsymbol{\mu}_{0P}$. To simplify the energy denominators in the sum-over-states of eq A1, the conventional mean-excitation-energy-approximation[18,85] is invoked for the solvent excitation energies: every excitation energy F_P in the sum-over-states is replaced by the *average* excitation energy $\mathcal{F}_A$, which is taken to be equal to the *first ionization potential* I_A of the rare-gas atom A.[18] Furthermore, the chromophore excitation energies E_I, E_J are approximated by the differences of the corresponding SCF orbital energies $\epsilon_a - \epsilon_i$ and $\epsilon_b - \epsilon_j$. This is also a crude approximation, neglecting two-electron contributions to excitation energies.

Combining everything we obtain eqs 9, 10, and 11 of section V.3. The polarizability of the chromophore is written as the second-order sum-over-states expression (with the mean excitation energy approximation already applied[18,85])

$$\alpha_A = \alpha_A\mathbf{I} = \frac{2}{\mathcal{F}_A}\sum_{P>0}\boldsymbol{\mu}_{0P}\boldsymbol{\mu}_{0P} \quad (A7)$$

$\boldsymbol{\mu}_{0P}$ being the transition dipole moment of the P $\leftarrow$ 0 excitation of the rare-gas atom i. The electronic factor K_{mn} of eq 10 is given by the expression

$$K_{mn} = d_{ia}{}^{mn} + \frac{1}{2}\left[\sum_{j\neq i}^{occ}(d_{ij}{}^{mn} - d_{aj}{}^{mn}) + \sum_{b\neq a}^{virt}(d_{ba}{}^{mn} - d_{bi}{}^{mn})\right] \quad (A8)$$

with

$$d_{tu}{}^{mn} = \sum_{\mu,\nu\in m}\sum_{\lambda,\sigma\in n}\frac{C_{t\mu}C_{\mu\nu}C_{u\lambda}C_{u\sigma}}{\epsilon_u - \epsilon_t - \mathcal{F}_A}S_{\mu\nu}S_{\lambda\sigma} \doteq \frac{Q_{tu}{}^mQ_{tu}{}^n}{\epsilon_u - \epsilon_t - \mathcal{F}_A} \quad (A9)$$

Note that the only difference to the original SBEJ approach appears in eq A9. The overlap integrals $S_{\mu\nu}$ and $S_{\lambda\sigma}$ do not appear in the original SBEJ formalism.

As already mentioned before, the *transition monopoles*

$$Q_{tu}{}^m = \sum_{\mu,\nu\in m}C_{t\mu}C_{\mu\nu}S_{\mu\nu} \quad (A10)$$

and the corresponding orbital excitation energies, $\epsilon_u - \epsilon_t$, are obtained from a minimal basis set (STO-3G) SCF calculation on the chromophore M. The gross overestimation of these entities, due to the neglect of two-electron contributions, results in a systematic overestimation of the spectral shift $\delta\nu$. The use of large basis sets does not help much either, due to the deficiencies of the approximations in the model (i.e., neglect of three-center integrals). Following Shalev et al.[18] we scale

the shift calculated in eq 10 by a factor η, which is specific to each chromophore-solvent pair. η is chosen to reproduce the experimentally measured shift for the binary complex M−A and maintained for the larger clusters $M-A_n$. Moreover, due to the heavily exaggerated SCF orbital excitation energies (up to five times larger than the true excitation energy, E_J), it is necessary to scale the average excitation energy $\mathcal{F}_A$, taken as the ionization potential I_A of A, up to higher values, i.e., $\mathcal{F}_A = \kappa I_A$ with $\kappa > 1$. Fortunately, it turned out that there is hardly any sensitivity of the shift on κ (once one is "out of resonance" with the orbital excitation energies in the denominator of eq A9), apart from a linear dependence already covered by η. Therefore, η and κ can be considered as redundant. Thus, a value $\kappa = 3.5$ was used in all calculations, independent of the chromophore.

Appendix B. Test Calculations with the Modified SBEJ Model on Solvent Clusters

We have carried out a series of test calculations on argon solvent clusters $M-A_n$ of various sizes with different chromophores, in order to test the proper functioning of the modified SBEJ method described in Appendix A. We have used the chromophores tetracene, anthracene, perylene ($\pi^* \leftarrow \pi$), and *s*-tetrazine ($\pi^* \leftarrow$ n). The spectral shifts were calculated for optimized cluster geometries, obtained using an advanced simulated-annealing scheme.[86] The chromophore frame was kept frozen during the simulation, and the intermolecular interactions were modeled by an effective pair potential of the 6−12 Lennard-Jones type. The 6−12 form was used here for ready comparison with the literature—all other computations reported in this paper were based on a 6−9 function, as already stated. The potential parameters were taken from ref 18c (C−Ar, H−Ar) or obtained by utilization of the usual mixing rules (N−Ar for *s*-tetrazine). For clusters of larger size one usually finds that several energetically-close lying isomers coexist. The corresponding local minima were found by quenching with a simulated annealing procedure. Spectral shifts were obtained for the optimized minimal-energy cluster structures, fitting the empirical scaling parameter, η, to the experimental shift of the $n = 1$ (binary) complex. For chromophores undergoing $\pi^* \leftarrow \pi$ transitions (anthracene, tetracene, perylene), the computed solvent shifts for clusters $M-A_n$ ($n = 1,...,8$) are very close to those reported in the original SBEJ papers.[18] Computed shifts are in reasonable agreement with experiment for tetracene−Ar_n and perylene−Ar_n clusters. The systematic underestimation of the experimental red shifts for the anthracene−Ar_n system, reported in ref 18, persisted in the current approach. The scaling factors used here are somewhat smaller but comparable to those of ref 18, i.e., $\eta = 0.29$ instead of $\eta = 0.37$ for tetracene. For the *s*-tetrazine−Ar_n clusters (of primary concern here) the computed spectral shifts on the $\pi^* \leftarrow$ n type lowest electronic transition are compiled in Table 8, together with the corresponding intermolecular binding energies of the distinct isomers, obtained for the model potential mentioned above after minimization. The related experimental values[74] are also given in Table 8 for comparison. Unfortunately, only non-mass-selective fluorescence excitation spectra of clusters with $n \leq 4$ are available at present. To assess the spectral shift of *s*-tetrazine in an argon matrix, a low energy configuration of a relatively large cluster ($n = 14$) was generated. The predicted red shift amounts to -350 cm^{-1}. We note here that the scaling parameter η, required to match the experimental $n = 1$ red shift of -23 cm^{-1}, is equal to 0.66. This value is substantially larger than those required for systems with $\pi^* \leftarrow \pi$ type transitions. However, as seen in Table 8, the agreement between measured and computed shifts after scaling is very satisfactory.

JA944087Y